The Nitrification Inhibitor Methyl 3-(4-Hydroxyphenyl) Propionate Modulates Root Development by Interfering with Auxin Signaling via the NO/ROS Pathway[1]

Yangyang Liu[2], Ruling Wang[2], Ping Zhang, Qi Chen, Qiong Luo, Yiyong Zhu, and Jin Xu*

Key Laboratory of Tropical Plant Resources and Sustainable Use, Xishuangbanna Tropical Botanical Garden, Chinese Academy of Sciences, Menglun, Mengla, Yunnan 666303, China (Y.L., R.W., P.Z., Q.L., J.X.); Faculty of Life Science and Technology, Kunming University of Science and Technology, Kunming 650500, China (Q.C.); and College of Resources and Environmental Sciences, Nanjing Agricultural University, Nanjing 210095, China (Y.Z.)

ORCID IDs: 0000-0003-3103-162X (Q.C.); 0000-0002-2335-0252 (Q.L.); 0000-0003-2695-8199 (Y.Z.); 0000-0002-1994-631X (J.X.).

Methyl 3-(4-hydroxyphenyl)propionate (MHPP) is a root exudate that functions as a nitrification inhibitor and as a modulator of the root system architecture (RSA) by inhibiting primary root (PR) elongation and promoting lateral root formation. However, the mechanism underlying MHPP-mediated modulation of the RSA remains unclear. Here, we report that MHPP inhibits PR elongation in Arabidopsis (*Arabidopsis thaliana*) by elevating the levels of auxin expression and signaling. MHPP induces an increase in auxin levels by up-regulating auxin biosynthesis, altering the expression of auxin carriers, and promoting the degradation of the auxin/indole-3-acetic acid family of transcriptional repressors. We found that MHPP-induced nitric oxide (NO) production promoted reactive oxygen species (ROS) accumulation in root tips. Suppressing the accumulation of NO or ROS alleviated the inhibitory effect of MHPP on PR elongation by weakening auxin responses and perception and by affecting meristematic cell division potential. Genetic analysis supported the phenotype described above. Taken together, our results indicate that MHPP modulates RSA remodeling via the NO/ROS-mediated auxin response pathway in Arabidopsis. Our study also revealed that MHPP significantly induced the accumulation of glucosinolates in roots, suggesting the diverse functions of MHPP in modulating plant growth, development, and stress tolerance in plants.

Nitrogen fertilizer is one of the most expensive nutrients to supply (Fan et al., 2009). Nitrification results in the transformation of ammonium to nitrate via nitrite in a reaction that is mediated by ammonia-oxidizing bacteria. However, nitrogen can be lost through the leaching of nitrate and gaseous nitrogen emissions, with potential adverse effects on the environment and human health (Subbarao et al., 2013). The low efficiency of agronomic nitrogen application is largely the result of nitrogen loss associated with nitrification and denitrification (Schlesinger, 2009; Subbarao et al., 2013). High levels of nitrification can lead to nitrogen starvation, which in turn forces plants to develop strategies to reduce nitrogen loss (Subbarao et al., 2013). Some plants, such as *Brachiaria* spp. grasses, have developed mechanisms to suppress nitrification via the exudation of specific secondary organic compounds from roots; this process is termed biological nitrification inhibition (BNI). Zakir et al. (2008) found that the root exudates of sorghum (*Sorghum bicolor*) possess BNI activity, and a subsequent study confirmed that BNI activity was attributable to multiple components present in the sorghum exudate and identified the isolated phenolic substance methyl 3-(4-hydroxyphenyl)propionate (MHPP) as the main active compound (Nardi et al., 2013). NH_4^+ induced greater MHPP production in plants (56.6 μM g^{-1} root dry weight d^{-1}) than standard Hoagland medium alone (17 μM g^{-1} root dry weight d^{-1}; Zakir et al., 2008). Although MHPP has been demonstrated to inhibit

[1] This work was supported by the China National Natural Sciences Foundation (grant nos. 31170228, 31272239, and 31172035), the Key Project of the State Key Laboratory of Desert and Oasis Ecology, Xinjiang Institute of Ecology and Geography of the Chinese Academy of Sciences, Yunnan Province Foundation for Academic Leaders (grant no. 2014HB043), the Knowledge Innovation Program of the Chinese Academy of Sciences (grant no. KSCX2–EW–Z–15), the Hebei Province National Natural Sciences Foundation for Distinguished Young Scientists (grant no. C2013503042), and the Program for New Century Excellent Talents in University (grant no. NCET–11–0672).

[2] These authors contributed equally to the article.

* Address correspondence to xujin@xtbg.ac.cn.

The author responsible for distribution of materials integral to the findings presented in this article in accordance with the policy described in the Instructions for Authors (www.plantphysiol.org) is: Jin Xu (xujin@xtbg.ac.cn).

J.X. conceived the original screening and research plans; J.X. and Y.L. supervised the experiments; Y.L. and R.W. performed most of the experiments; R.W., P.Z., Q.L., Q.C., and Y.Z. provided technical assistance to Y.L.; J.X. and Y.L. designed the experiments and analyzed the data; J.X. conceived the project and wrote the article with contributions of all the authors; J.X. supervised and complemented the writing.

www.plantphysiol.org/cgi/doi/10.1104/pp.16.00670

nitrification, no further studies have been undertaken to characterize the effect of MHPP as a root exudate on plant growth and root system development.

Root system growth and development are complex processes that are modulated by a variety of phytohormones and signaling molecules, including auxin, ethylene, abscisic acid (ABA), nitric oxide (NO), and reactive oxygen species (ROS), as well as their interactions (Van de Poel et al., 2015). Auxin plays a central role in regulating root growth by positioning the stem cell niche, controlling division of the meristem, and increasing cell volume in the elongation zone via the modulation of auxin biosynthesis, transport, and responses (Wang et al., 2009). Maintaining a maximal auxin concentration in the quiescent center (QC) and a steep auxin gradient in the proximal meristem, which decreases with increasing distance from the QC, is required for normal root growth (Laskowski et al., 2008). The auxin influx carriers in the AUXIN1/LIKE AUX1 (AUX1/LAX) family and efflux carriers in the PIN-FORMED (PIN) family mediate polar auxin transport (PAT) in plants and subsequent root system architecture (RSA) remodeling in response to environmental cues, including biotic and abiotic stresses. Different auxin carriers can modulate a common physiological process or stress response via various signaling pathways. For example, both PIN2 and AUX1 are required for plant adaptation to alkaline stress. PIN2 induces alkaline stress adaptation via a PKS5-mediated signaling cascade to modulate proton secretion in root tips to maintain primary root (PR) elongation (Xu et al., 2012; Li et al., 2015). AUX1 is involved in alkaline stress-induced RSA remodeling via ethylene-mediated auxin accumulation (Li et al., 2015). Additionally, AUX1 and PIN2 sustain lateral root (LR) formation in Arabidopsis (*Arabidopsis thaliana*) during the early stages of iron (Fe) toxicity (Li et al., 2015).

NO has been identified as an important signaling molecule that interplays with ROS in response to stresses and in the regulation of root growth. NO protects plant cells against oxidative stress by reducing ROS accumulation (Wink and Mitchell, 1998; Xu et al., 2010a). The NO biosynthesis-related mutant *nitric oxide-associated1* (*noa1*) exhibits reduced PR elongation in association with increased ROS accumulation. Our previous study indicated that zinc (Zn) toxicity-induced NO accumulation increased the ROS level in *Solanum nigrum* roots by modulating the expression and activity of antioxidative enzymes and that this elevation of ROS production resulted in programmed cell death in root tips; thus, NO modulates the RSA and the subsequent adaptation of the RSA in response to Zn stress (Xu et al., 2010a).

Synergistic effects of NO and auxin on a series of plant responses have been observed. Exogenous auxin application increased NO production (Correa-Aragunde et al., 2004; Lombardo et al., 2006), and NO accumulation in roots mediates auxin-induced LR formation (Correa-Aragunde et al., 2004), adventitious root growth (Tewari et al., 2008), and root hair development (Lombardo et al., 2006). Our previous study indicated that NO elevates the indole-3-acetic acid (IAA) level in cadmium-treated *Medicago* spp. roots by reducing its degradation via IAA oxidase activity, thereby promoting auxin equilibrium and ameliorating cadmium toxicity (Xu et al., 2010b). Fernández-Marcos et al. (2011) found that a high NO level inhibits root-ward auxin transport in Arabidopsis roots by reducing the abundance of PIN1. Terrile et al. (2012) found that *S*-nitrosylation of the auxin receptor TIR1 promotes its interaction with auxin/IAA (Aux/IAA) proteins, which are transcriptional repressors of genes associated with auxin responses. The NO biosynthesis-related triple mutant *nitrate reductase1* (*nia1*)/*nia2*/*noa1* exhibits reduced NO levels and small root meristems with abnormal divisions. Further investigation indicated that the abnormal phenotypes of this NO mutant are related to perturbations in auxin biosynthesis, transport, and signaling (Sanz et al., 2014).

Similar to NO, ROS also might regulate root growth and development by modulating auxin homeostasis and signaling. The expression of auxin-responsive genes is decreased by hydrogen peroxide (H_2O_2) treatment via mitogen-activated protein kinase activation (Kovtun et al., 2000). Defects in antioxidative capacity caused by simultaneous thioredoxin and glutathione mutation result in altered auxin homeostasis and development (Bashandy et al., 2010). Blomster et al. (2011) found that apoplastic ozone transiently suppressed auxin signaling by reducing the gene expression levels of auxin receptors and Aux/IAA family transcriptional repressors. However, auxin receptor mutants are more tolerant to H_2O_2 (Iglesias et al., 2010); therefore, reducing the expression of auxin receptor genes might be an adaptive mechanism by which plants respond to ROS accumulation.

Here, we report that MHPP, in addition to its function as a nitrification inhibitor, acts as an important regulator of the RSA by inhibiting PR elongation and promoting LR formation in Arabidopsis seedlings by regulating the auxin levels in the root tip and modulating meristematic cell division potential. We found that exogenous MHPP increased the levels of auxin signaling by promoting the expression of IAA biosynthesis-related genes, increasing auxin perception via the destabilization of Aux/IAA, and significantly repressing the expression of PIN4 in root tips. Furthermore, MHPP-induced NO production promoted an increase in ROS accumulation in root tips, and inhibition of NO/ROS accumulation ameliorated the MHPP-induced reduction in PR growth. Genetic analysis supported the phenotype described above. Our study also revealed that MHPP significantly induced the accumulation of glucosinolates in roots. The potential mechanisms involved in this process are discussed.

RESULTS

Effects of MHPP on PR Development

Previous studies indicated that the root exudate MHPP exerts a significant inhibitory effect on nitrification in soil. To further explore whether MHPP could modulate

root system development, 5-d-old Arabidopsis seedlings germinated on one-half-strength Murashige and Skoog (MS) plates were transferred to new plates supplemented with or without 40 or 80 μM MHPP for continued growth for 5 d, and the PR growth and LR number were measured. PR elongation was inhibited and LR number was increased in the presence of either 40 or 80 μM MHPP, and these effects were positively associated with the MHPP concentration (Fig. 1, A, B, and F). Specifically, PR elongation was inhibited by 25% and 46% in seedlings exposed to 40 and 80 μM MHPP, respectively (Fig. 1B). The LR number was increased by 158% and 205% following exposure to 40 and 80 μM MHPP, respectively (Fig. 1F). To further explore the effect of MHPP on LR formation, we analyzed lateral root primordium (LRP) initiation. As shown in Figure 1G, LRP initiation was enhanced in all four stages following exposure to 40 or 80 μM MHPP. To examine the inhibitory effects of MHPP on PR elongation in detail, we also measured the lengths of meristem zones and elongation zones in the MHPP-treated roots. As shown in Figure 1, C and D, the lengths of both meristem zones and elongation zones were decreased in roots exposed to 40 or 80 μM MHPP. MHPP treatment also reduced the average cell length in the differentiation zone (Fig. 1E).

PR growth inhibition can be caused by reductions in stem cell niche activity and meristematic cell division potential in root tips (Baluska et al., 2010; Li et al., 2015). Therefore, we first analyzed the possible change in stem cell activity using the QC-specific marker *QC25*:*GUS* (Sabatini et al., 1999). GUS staining in the QC showed a similar expression pattern between control- and MHPP-treated roots (Supplemental Fig. S1, A and D). *PLETHORA* (*PLT*) acts in concert with *SHORT ROOT* (*SHR*) to control QC identity (Sabatini et al., 1999). Thus, we next analyzed the influence of MHPP on the expression of PLT1 and SHR. Examination of *PLT1pro*:*PLT1-GFP* and *SHRpro*:*SHR-GFP* activities indicated that the expression levels of both the PLT1 and SHR reporters were unaltered in MHPP-treated roots compared with the control-treated roots (Supplemental Fig. S1, B, C, E, and F).

We next examined meristematic cell division potential in a transgenic line expressing *CYCB1;1*:*GUS*, a marker used to monitor cell cycle progression (Colón-Carmona et al., 1999). Histochemical staining showed that GUS activity was dramatically higher in MHPP-treated roots than in control-treated roots (Fig. 1, H and I; Supplemental Fig. S1G). It is known that *CYCB1;1* transcription is activated during G2 phase and that CYCB1;1 is degraded at metaphase (Zheng et al., 2011). The increased accumulation of CYCB1;1 suggests that cell cycle progression was hampered at the G2-to-M phase transition. These data indicated that MHPP inhibited PR growth by affecting meristematic cell division potential.

The above results show that MHPP inhibited PR elongation while increasing LR number, thereby modulating the RSA. The root system is the major organ through which plants absorb nutrient elements. Thus, we examined the nutrient element contents in seedlings. Inductively coupled plasma-mass spectrometry analysis indicated that MHPP treatment markedly increased the contents of phosphorus (P), sulfur (S), Fe, manganese (Mn), and Zn and slightly increased the potassium (K) and copper (Cu) contents in seedlings (Fig. 1J). These data indicated that MHPP improved nutrient element accumulation in plants.

Auxin Is Involved in the MHPP-Mediated Inhibition of PR Meristem Development

Auxin plays an essential role in root system development and root meristem maintenance (Overvoorde et al., 2010). The altered RSA and root meristem patterning observed in MHPP-treated seedlings raised the question of whether the auxin content is affected by MHPP. Therefore, we measured the IAA level in MHPP-treated roots using gas chromatography-mass spectrometry (GC-MS) and found that the IAA level was higher in MHPP-treated roots than in control-treated roots (Fig. 2A). We then tested the hypothesis that MHPP affects auxin signaling in the root apical meristem. For this purpose, we used seedlings expressing the auxin-responsive marker *DR5*:*GFP*. Seedlings were grown on one-half-strength MS medium for 5 d, followed by treatment with or without 40 or 80 μM MHPP for up to 24 h, during which GFP fluorescence was monitored. MHPP indeed increased the expression of the auxin reporter in root tips until 12 h, but the expression of this reporter returned to the control level after 24 h of treatment (Fig. 2, B and C; Supplemental Fig. S2, A and B).

To investigate how MHPP increased the auxin levels, we conducted quantitative reverse transcription (qRT)-PCR analysis to estimate the transcript levels of the genes that encode key enzymes in the auxin biosynthesis pathway. Consistent with the finding of increased IAA levels in roots, the qRT-PCR results revealed that MHPP significantly increased the transcript levels of many IAA biosynthesis genes, including *ASA1*, *PAT1*, *AMI1*, *SUR1*, *TAA1*, *YUC2*, *YUC3*, *YUC9*, *AAO1*, and *AAO3*, in Arabidopsis seedlings (Fig. 2D). These results suggest that MHPP up-regulates IAA biosynthesis gene expression, which influences the auxin content in roots, and that an increased auxin level may be responsible for the reduction in PR growth in MHPP-treated seedlings. We tested this hypothesis by exogenously applying auxin. Five-day-old seedlings germinated in one-half-strength MS medium were transferred to fresh one-half-strength MS medium containing 40 or 80 μM MHPP supplemented with 0.5 nM IAA, and PR elongation was measured 2 d after transfer. As shown in Figure 2E, application of IAA further repressed PR growth in seedlings subjected to MHPP treatment. To confirm that elevated IAA expression is involved in the MHPP-induced inhibition of PR growth, we analyzed the root growth of *yucca*, an auxin-overproducing mutant (Zhao et al., 2001), during MHPP treatment. The *yucca* mutant

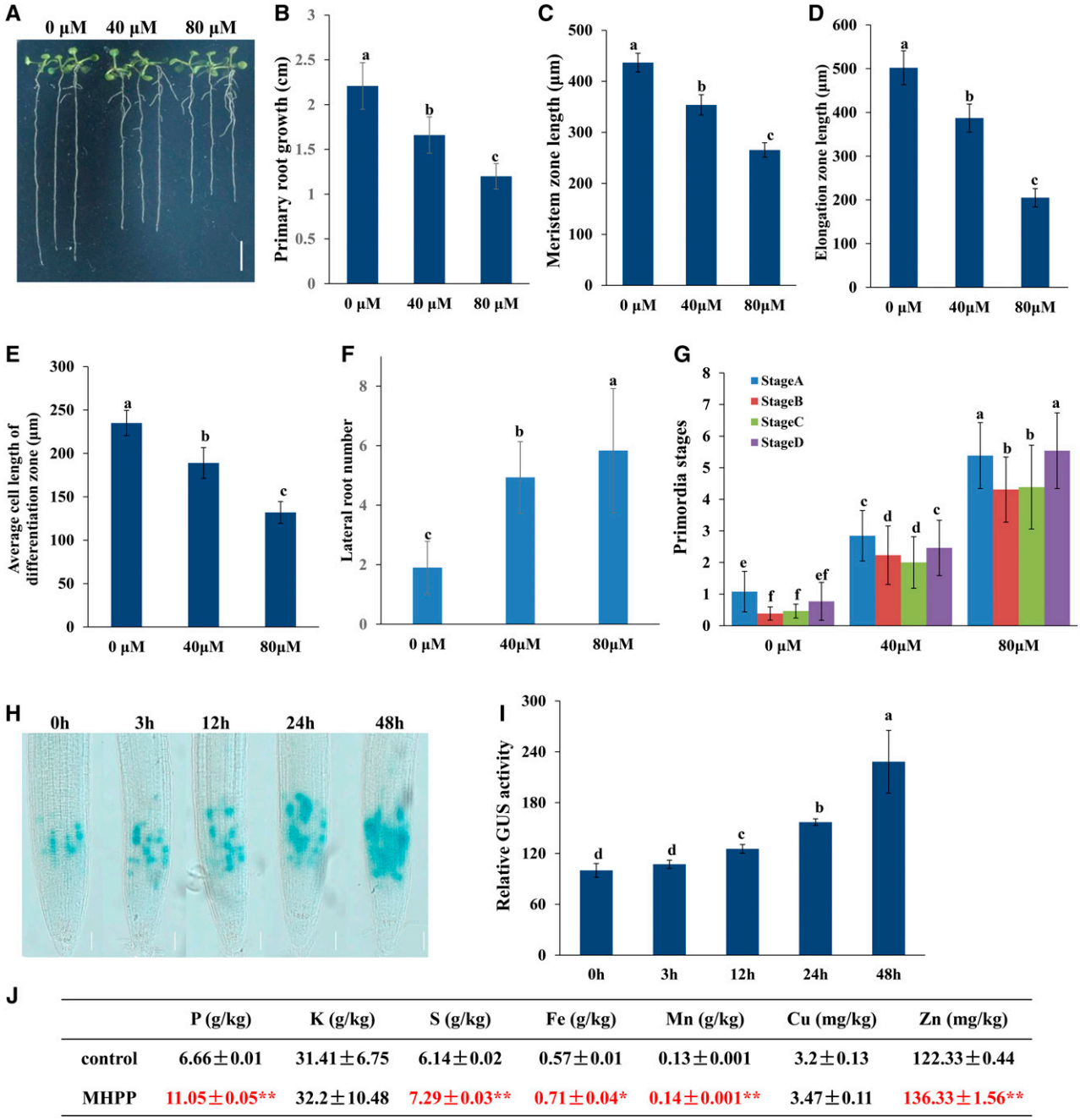

J

	P (g/kg)	K (g/kg)	S (g/kg)	Fe (g/kg)	Mn (g/kg)	Cu (mg/kg)	Zn (mg/kg)
control	6.66±0.01	31.41±6.75	6.14±0.02	0.57±0.01	0.13±0.001	3.2±0.13	122.33±0.44
MHPP	11.05±0.05**	32.2±10.48	7.29±0.03**	0.71±0.04*	0.14±0.001**	3.47±0.11	136.33±1.56**

Figure 1. MHPP affected root system development in Arabidopsis. A to G, Five-day-old wild-type seedlings grown in one-half-strength MS medium were treated with 40 or 80 μM MHPP for 5 d (A). Bar = 0.5 cm. PR elongation (B), the lengths of meristem zones (C) and elongation zones (D), the average cell length in the differentiation zone (E), the number of lateral roots (F), and LRP initiation (G) were measured after 5 d of treatment. H and I, Image of GUS staining in 5-d-old *CYCB1;1*:*GUS* seedlings exposed to 40 μM MHPP for 3 to 48 h (H) and relative GUS activity of *CYCB1;1*:*GUS* seedlings (I) treated as in H. Bars = 50 μm. The level of GUS activity in untreated roots was set to 100. Error bars represent the SE. Different letters indicate significantly different values ($P < 0.05$ by Tukey's test). J, Nutrient element contents in MHPP-treated Arabidopsis seedlings. The ± values represent the SE. Asterisks indicate significant differences with respect to the corresponding control based on Tukey's test (*, $0.01 < P < 0.05$; and **, $P < 0.01$).

seedlings accumulated higher IAA levels in roots (Fig. 2A) and exhibited much shorter PR elongation than wild-type seedlings (Fig. 2, F and G). These data indicated that MHPP inhibited PR elongation by increasing auxin accumulation via increased expression of auxin biosynthesis-related genes.

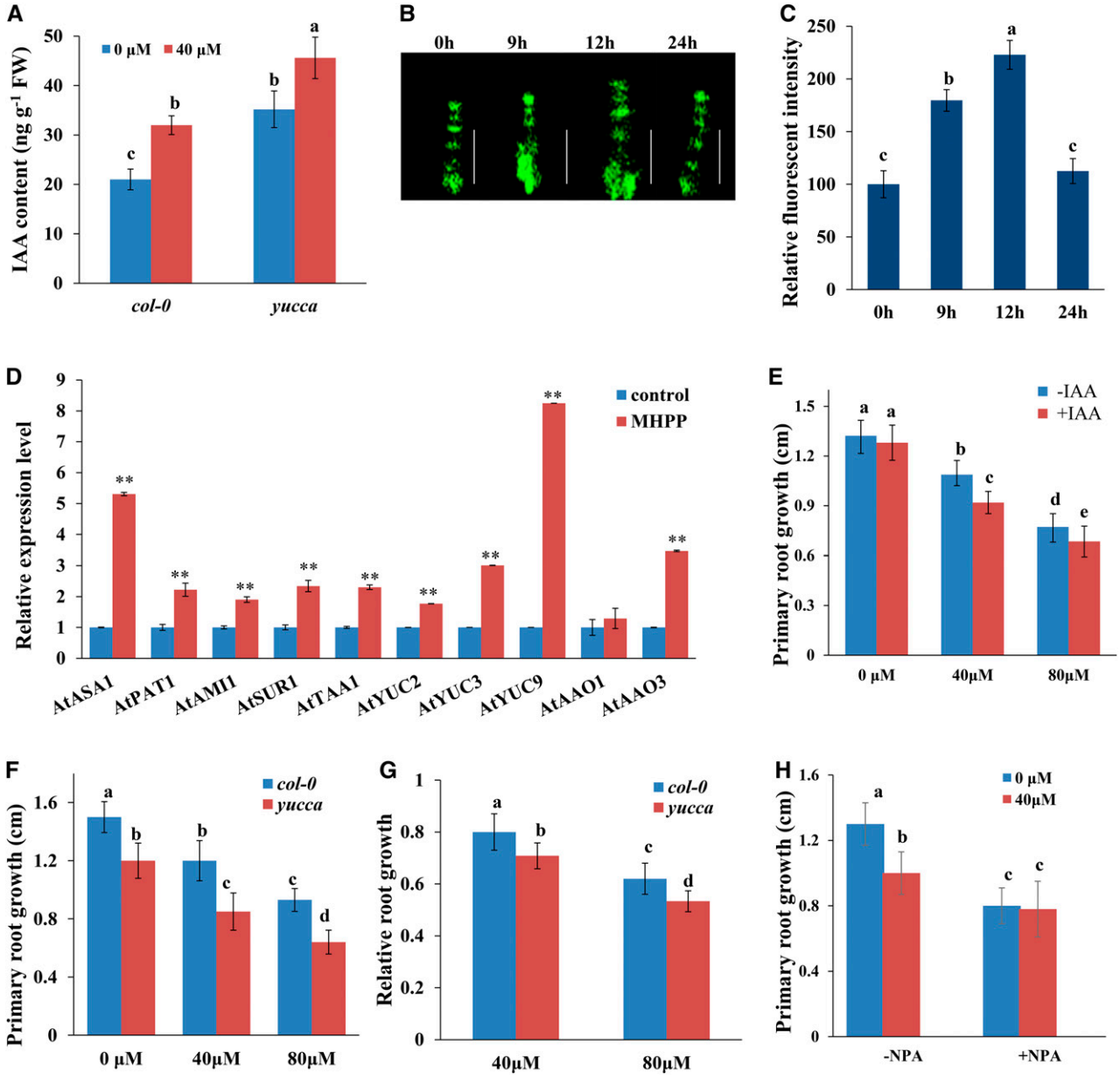

Figure 2. MHPP treatment enhanced auxin accumulation in roots, thus inhibiting PR growth. A, IAA contents in the roots of Columbia-0 (Col-0) and *yucca* seedlings treated with or without 40 μM MHPP for 24 h. FW, Fresh weight. B and C, GFP fluorescence in roots of 5-d-old *DR5:GFP* seedlings exposed to 40 μM MHPP for 9 to 24 h (B) and quantification of *DR5:GFP* fluorescence intensity (C) in plants treated as in B. The fluorescence intensity of untreated roots was set to 100. Bars = 50 μm. D, qRT-PCR analysis of the expression of auxin biosynthesis-related genes in Col-0 seedlings treated with or without 40 μM MHPP for 12 h. The expression levels of the indicated genes in untreated roots were set to 1. E, PR growth of Col-0 seedlings treated with or without MHPP (40 or 80 μM) in the presence of 0 or 0.5 nM IAA for 2 d. F and G, PR growth of Col-0 and *yucca* seedlings treated with or without MHPP (40 or 80 μM) for 2 d (F) and relative root growth of seedlings of the two genotypes treated with 40 or 80 μM MHPP compared with untreated seedlings (G). H, PR growth of wild-type seedlings treated with or without 40 μM MHPP in the presence or absence of 1 μM NPA for 2 d. Error bars represent the SE. Asterisks indicate significant differences with respect to the corresponding control (**, $P < 0.01$ based on Tukey's test). Different letters indicate significantly different values ($P < 0.05$ by Tukey's test).

PAT plays a role in auxin accumulation and distribution in root tips. The MHPP-induced changes in auxin levels in root tips may result from changes in PAT. We thus examined the effects of naphthylphthalamic acid (NPA), an auxin transport inhibitor, on the MHPP-induced inhibition of PR elongation. Although MHPP treatment alone decreased PR growth, PR elongation was not reduced further by the addition of NPA (Fig. 2H). This result suggests that PAT is responsible for the modulation of PR growth in MHPP-treated seedlings.

PIN4 Is Required for the MHPP-Induced Inhibition of PR Growth

The above results show that PAT is required for the MHPP-induced inhibition of PR growth. PAT is mediated by auxin influx carriers in the AUX/LAX family and efflux carriers in the PIN family (Péret et al., 2012; Yuan et al., 2014; Yuan and Huang, 2016). Thus, we examined whether MHPP treatment also affects the expression of auxin carriers in roots. We first analyzed the gene expression levels of *AUX1*, *PIN1*, *PIN2*, *PIN4*, and *PIN7* in MHPP-treated roots. As shown in Figure 3A, MHPP treatment significantly reduced the expression levels of *PIN4* and slightly reduced the expression of *PIN1* and *PIN2* compared with the control treatment, whereas the gene expression levels of *AUX1* and *PIN7* were nearly unaffected. We then analyzed the expression levels of AUX1, PIN1, PIN2, PIN4, and PIN7 proteins in MHPP-treated roots using transgenic lines expressing *AUX1*:*YFP*, *PIN1*:*GFP*, *PIN2*:*GFP*, *PIN4*:*GFP*, and *PIN7*:*GFP*. As visualized by yellow fluorescent protein (YFP) or GFP fluorescence, following exposure to MHPP, the expression level of PIN4:GFP was reduced markedly. However, there were no visible differences in the changes in the cell type/tissue expression pattern of PIN4:GFP or in its membrane localization between MHPP and control treatment (Fig. 3, B and C; Supplemental Fig. S2, C and D). However, the expression levels of AUX1, PIN1, PIN2, and PIN7 were unaffected (Supplemental Fig. S3). These results suggest that PIN4 is involved in the MHPP-induced changes in auxin accumulation and distribution in root tips.

We next investigated the roles of these auxin carriers in the MHPP-induced inhibition of PR growth using *aux1* and *pin* mutants. Whereas *aux1-21*, *pin1*, *pin2*, and *pin7-2* seedlings exhibited similar phenotypes to wild-type seedlings (Supplemental Fig. S4), *pin4-3* seedlings exhibited a less extensive reduction in PR elongation in response to MHPP treatment (Fig. 3, D and E). These results suggest that the MHPP-mediated inhibition of PR elongation via the regulation of auxin distribution is predominantly modulated by PIN4.

MHPP Enhances Auxin Perception by Destabilizing Aux/IAA

The above results show that MHPP increased auxin distribution in root tips. To determine whether the effects of MHPP on the DR5:GFP signal involve auxin perception changes, we examined the effects of α-(*p*-chlorophenoxy)isobutyric acid (PCIB), which inhibits auxin signaling by stabilizing native Aux/IAA proteins

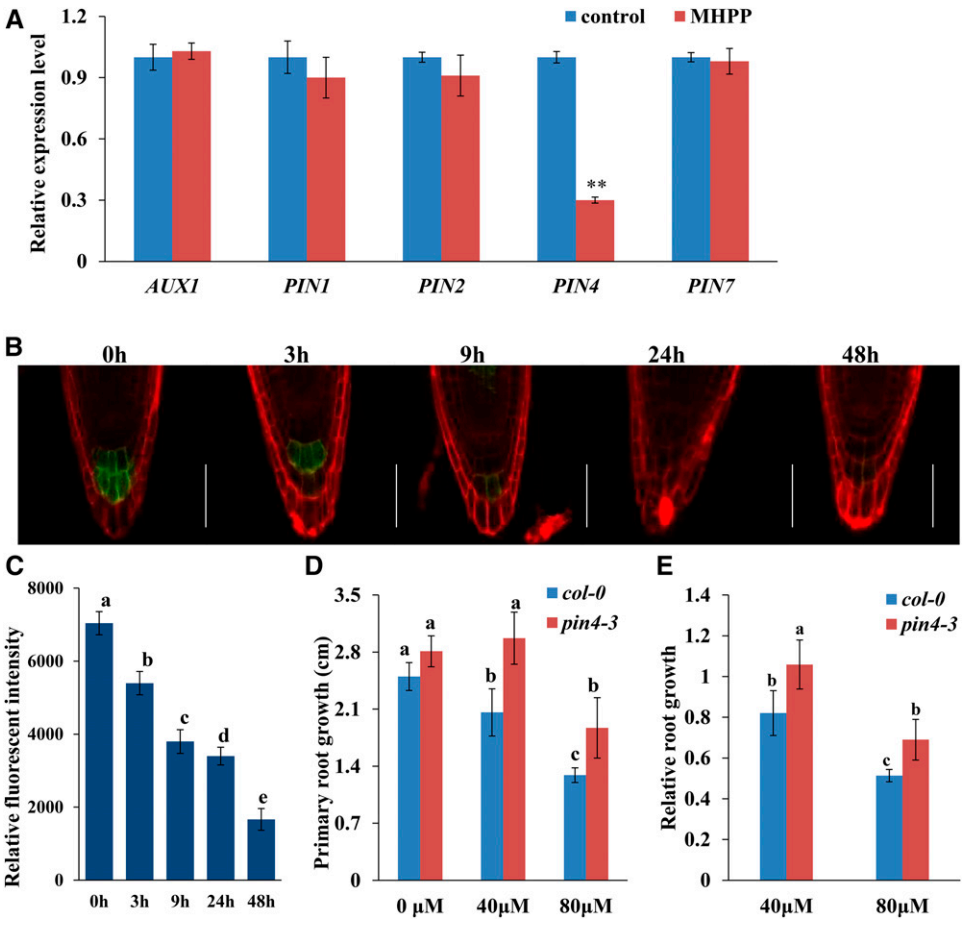

Figure 3. PIN4 plays a role in the MHPP-mediated inhibition of PR growth. A, qRT-PCR analysis of the expression of auxin carrier genes in the roots of Col-0 seedlings treated with or without 40 μM MHPP for 12 h. The expression levels of the indicated genes in untreated roots were set to 1. B and C, GFP fluorescence in the roots of 5-d-old *PIN4*:*GFP* seedlings exposed to 40 μM MHPP for 3 to 48 h (B) and quantification of the *PIN4*:*GFP* fluorescence intensity (C) in plants treated as in B. Bars = 50 μm. D and E, PR growth of Col-0 and *pin4-3* seedlings treated with or without MHPP (40 or 80 μM) for 2 d (D) and relative root growth of seedlings of the two genotypes treated with 40 or 80 μM MHPP compared with untreated seedlings (E). Error bars represent the SE. Asterisks indicate a significant difference with respect to the corresponding control (**, $P < 0.01$ based on Tukey's test). Different letters indicate significantly different values ($P < 0.05$ by Tukey's test).

(Oono et al., 2003), on the MHPP-induced inhibition of PR elongation. Although MHPP treatment alone decreased PR growth, PR elongation was not reduced further by the addition of PCIB (Fig. 4A). These results suggest that Aux/IAA proteins are responsible for the modulation of PR growth in MHPP-treated seedlings.

We next used a transgenic line expressing the VENUS protein fused to Aux/IAA-auxin interaction domain II (*DII-VENUS*; Brunoud et al., 2012). In this transgenic line, the VENUS signal is sensitive to auxin in a dose-dependent manner, without disrupting the activity of the auxin response machinery (Brunoud et al., 2012). Five-day-old *DII-VENUS* seedlings were treated with MHPP, and YFP fluorescence was monitored. Treatment with MHPP resulted in rapid degradation of the nuclear DII-VENUS fluorescent signal but did not alter

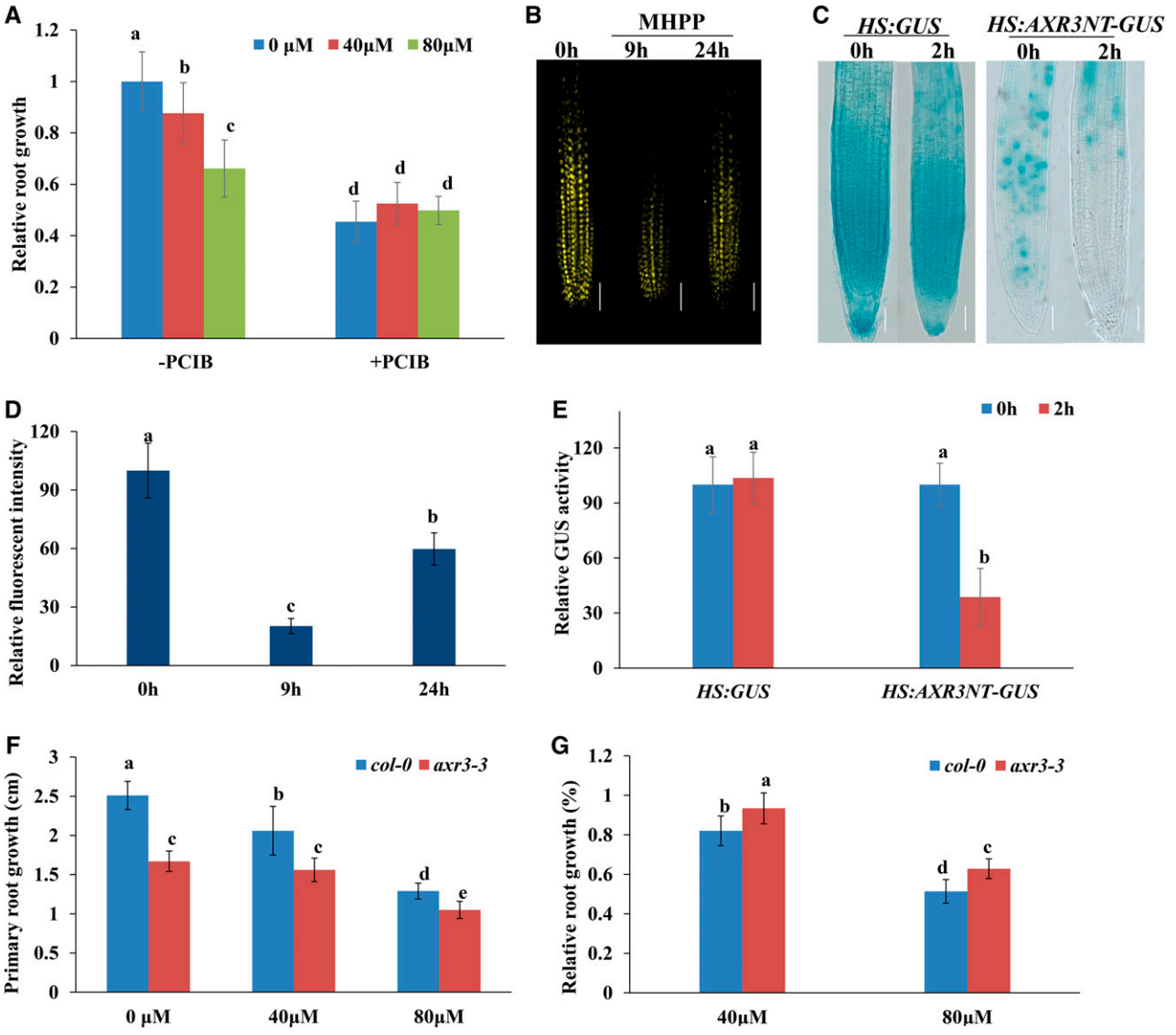

Figure 4. MHPP treatment reduces the stability of Aux/IAA proteins. A, Relative root growth of wild-type seedlings treated with MHPP (40 or 80 μM) in the presence or absence of 100 μM PCIB for 2 d. The length of untreated roots of Col-0 plants was set to 1. B and D, YFP fluorescence in roots of 5-d-old *DII-VENUS* seedlings exposed to 40 μM MHPP for 9 or 24 h (B) and quantification of *DII-VENUS* fluorescence intensity (D) in plants treated as in B. The fluorescence intensity of untreated roots was set to 100. Bars = 50 μm. C, GUS staining of 5-d-old *HS:AXR3NT-GUS* seedlings. The seedlings were heat shocked at 37°C for 2 h and then treated with or without 40 μM MHPP for 45 min at 23°C, followed by GUS staining. Bars = 50 μm. E, Relative GUS activity of *HS:AXR3NT-GUS* seedlings treated as in C. The level of GUS activity in untreated roots was set to 100. F and G, PR growth of Col-0 and *axr3-3* seedlings treated with or without MHPP (40 or 80 μM) for 2 d (F) and relative root growth of seedlings of the two genotypes treated with 40 or 80 μM MHPP compared with untreated seedlings (G). Error bars represent the SE. Different letters indicate significantly different values ($P < 0.05$ by Tukey's test).

the expression of the auxin-insensitive reporter *mDII-VENUS* (Fig. 4, B and D; Supplemental Fig. S5). These results suggest that MHPP enhances IAA perception in root tips. To confirm the effect of MHPP on Aux/IAA degradation, we used the *HS:AXR3-GUS* reporter line, which harbors a construct coding for the N terminus of the Aux/IAA protein AXR3/IAA17 and the GUS reporter under the control of a heat shock-inducible promoter (Gray et al., 2001). After heat shock, the AXR3-GUS signal decreased significantly in MHPP-treated seedlings (Fig. 4, C and E). Therefore, we hypothesize that MHPP up-regulates the auxin signaling pathway upstream of the ubiquitin-mediated degradation of Aux/IAA proteins.

To verify that Aux/IAA proteins are involved in the MHPP-induced inhibition of PR growth, we analyzed PR elongation in gain-of-function *axr3-3* mutant seedlings upon MHPP treatment (Rouse et al., 1998). The mutant seedlings exhibited less extensive suppression of PR growth in the presence of MHPP than control seedlings (Fig. 4, F and G). These results indicate that MHPP treatment inhibits PR growth by amplifying auxin signaling in root tips by destabilizing Aux/IAA proteins.

Involvement of NO and ROS in the MHPP-Mediated Inhibition of PR Growth

To assess the correlation between NO/ROS accumulation and MHPP treatment, we measured NO and ROS levels in MHPP-treated seedlings. To visualize NO and ROS localization in roots, we used a NO-specific fluorescent probe, 4,5-diaminofluorescein diacetate (DAF-2 DA), and a ROS-specific fluorescent probe, 2,7-dichlorofluorescein diacetate (DCFH-DA). MHPP treatment induced a marked increase in NO and ROS marker fluorescence intensity from the meristem zone to the elongation zone of roots (Fig. 5, A and B; for representative images, see Supplemental Fig. S6, A and B). Supplementation with the NO scavenger cPTIO or the NO synthase inhibitor L-NAME markedly inhibited the production of ROS in roots compared with MHPP treatment alone (Supplemental Fig. S7, A and B). In contrast, supplementation with the ROS scavenger potassium iodide (KI) did not alter NO levels in MHPP-treated roots (Supplemental Fig. S7, C and D). To confirm that MHPP-induced NO production increases ROS levels, we analyzed the ROS levels in *noa1*, a NO-deficient mutant, upon MHPP treatment. MHPP-induced NO accumulation was reduced markedly in *noa1* mutant roots compared with Col-0 roots (Fig. 5, C and D). Similarly, both ROS fluorescence and DAB staining analysis indicated that MHPP-induced ROS accumulation also was reduced markedly in *noa1* mutant roots compared with Col-0 roots (Fig. 5, E and F; Supplemental Fig. S8). These data suggest that MHPP induces NO production upstream of ROS accumulation in roots.

To investigate the physiological mechanisms underlying the roles of NO in MHPP-mediated PR growth inhibition, 5-d-old seedlings were treated with 40 or 80 μM MHPP in the presence or absence of SNP, cPTIO, or L-NAME. As shown in Figure 6, A to F, in the presence of the NO donor SNP, the PRs of seedlings were shorter, whereas in the presence of cPTIO or L-NAME, the PRs of seedlings were longer than those of seedlings exposed to MHPP alone at 2 d of treatment. We next analyzed PR growth in the *noa1* mutant upon MHPP treatment. Consistent with the results obtained from the pharmacological assay, *noa1* exhibited a less extensive reduction in PR elongation in the presence of 80 μM MHPP (Fig. 6, G and H). These results suggest that NO is involved in the MHPP-mediated inhibition of PR growth.

We subsequently explored the possible involvement of ROS in the signal transduction of MHPP-induced morphological responses. We examined PR elongation in 5-d-old seedlings treated with 40 or 80 μM MHPP in the presence or absence of H_2O_2 or the ROS scavenger KI or CATALASE (CAT) for 2 d. The MHPP-mediated repression of PR growth was more extensive in seedlings supplemented with H_2O_2 (Fig. 7, A and B) but was less extensive in seedlings supplemented with KI (Fig. 7, C and D) or CAT (Fig. 7, E and F). To verify the role of ROS in MHPP-mediated PR growth inhibition, ROS-deficient mutant lines also were examined. We found that the respiratory burst oxidase homolog mutants *rbohC* and *rbohD* and the double mutant *rbohD/F* exhibited a less extensive reduction in PR elongation than the wild-type Col-0 control in the presence of 80 μM MHPP (Fig. 8). These data indicate that MHPP treatment inhibits PR growth via NO-mediated ROS accumulation in root tips.

Based on the above results showing that MHPP inhibits PR growth by modulating meristematic cell division potential, we hypothesized that NO and ROS were involved in MHPP-induced inhibition of meristematic cell division potential. Thus, we examined the effects of NO/ROS on meristematic cell division potential using the *CYCB1;1:GUS* marker line. GUS staining showed that supplementation with the NO scavenger cPTIO, the NO synthase inhibitor L-NAME, or either ROS scavenger KI or CAT alleviated the overaccumulation of CYCB1;1 in roots caused by MHPP treatment (Fig. 9). However, supplementation with the NO donor SNP or H_2O_2 did not further increase CYCB1;1 accumulation in roots, perhaps because the MHPP-induced accumulation of NO and ROS in roots increased CYCB1;1 accumulation such that exogenous SNP or H_2O_2 application could not further enhance CYCB1;1 accumulation. These data indicate that NO and ROS are responsible for the MHPP-mediated inhibition of root meristem development.

NO-Mediated ROS Accumulation Was Possibly Responsible for MHPP-Induced Auxin Accumulation in Root Tips and the Inhibition of Root Meristem Development

The above results show that MHPP inhibits PR elongation by increasing auxin accumulation in root tips. To determine whether MHPP-induced NO and ROS accumulation is involved in this process, we used the

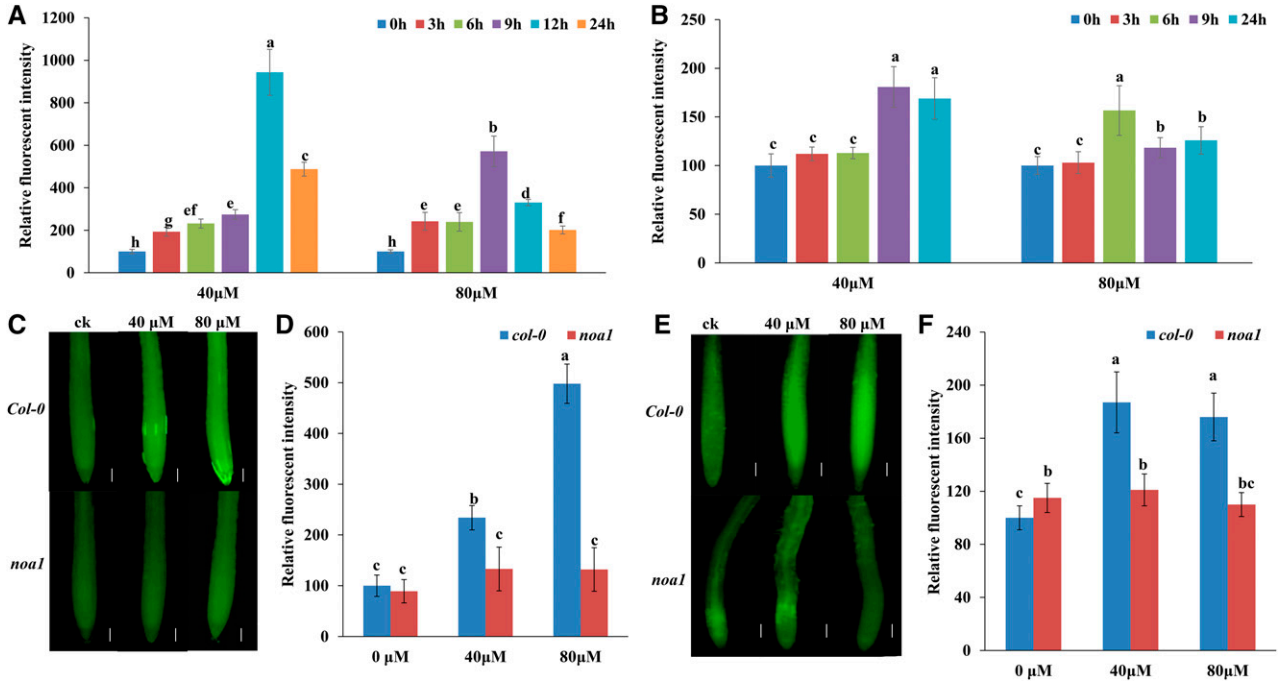

Figure 5. NO and ROS are involved in the MHPP-mediated inhibition of PR growth. A and B, Quantification of the NO-specific fluorescence intensity (A) and ROS-specific fluorescence intensity (B) in roots of Col-0 seedlings treated with MHPP (40 or 80 μM) for up to 24 h. The fluorescence intensity of untreated roots was set to 100. For representative images, see Supplemental Figure S6. C, NO contents in the roots of Col-0 and *noa1* seedlings treated with or without MHPP (40 or 80 μM) for 24 h, as revealed by the NO-specific fluorescent probe DAF-2 DA. Bars = 50 μm. D, Quantification of the NO-specific fluorescence intensity in plants treated as in C. E, ROS contents in the roots of Col-0 and *noa1* seedlings treated with or without MHPP (40 or 80 μM) for 24 h, as revealed by the ROS-specific fluorescent probe DCFH-DA. Bars = 50 μm. F, Quantification of the ROS-specific fluorescence intensity in plants treated as in E. Error bars represent the SE. Different letters indicate significantly different values ($P < 0.05$ by Tukey's test).

auxin-responsive *DR5*:*GFP* marker line to monitor the potential changes in auxin signaling in MHPP-treated seedlings in the presence or absence of an NO scavenger/inhibitor or an H_2O_2 scavenger. Exogenous addition of cPTIO or L-NAME reduced the expression of *DR5*:*GFP* in MHPP-treated seedlings. Similarly, the H_2O_2 scavenger KI or CAT reduced, whereas exogenous H_2O_2 increased, the expression of this auxin reporter in MHPP-treated seedlings (Fig. 10, A and B; for representative images, see Supplemental Figs. S9 and S10). To verify the role of NO/ROS in modulating auxin levels, we used the auxin-perceptive marker line *DII-VENUS*. Exogenous application of an NO scavenger/inhibitor (cPTIO or L-NAME) or an H_2O_2 scavenger (KI or CAT) stabilized, whereas SNP or H_2O_2 further reduced, the fluorescence of the DII-VENUS marker in MHPP-treated seedlings (Fig. 10, C and D; for representative images, see Supplemental Figs. S11 and S12). These data indicate that MHPP-induced NO acts as a second messenger to promote H_2O_2 production, thereby regulating root growth via the auxin pathway.

MHPP Induced the Accumulation of Glucosinolates in Arabidopsis Roots

To further investigate the role and molecular mechanisms of MHPP in modulating plant growth and development, we analyzed the transcript profiles in roots via high-throughput RNA sequencing (RNA-seq) followed by qRT-PCR analysis. We compared the transcripts obtained at 2 d in the presence of 40 or 80 μM MHPP. Relative to the gene expression levels under control conditions, 101 genes were down-regulated and 103 genes were up-regulated (altered by more than 2-fold) in roots treated with 40 μM MHPP, and 184 genes were down-regulated and 180 genes were up-regulated in roots treated with 80 μM MHPP ($\log_2 > 1$, false discovery rate < 0.01; Supplemental Fig. S13). The differentially expressed genes showed enrichment in the Kyoto Encyclopedia of Genes and Genomes pathway of glucosinolate biosynthesis due to either 40 or 80 μM MHPP treatment (Supplemental Figs. S14 and S15; Supplemental Table S1). We used qRT-PCR analysis to confirm the results of RNA-seq for the glucosinolate biosynthesis-related genes. The qRT-PCR analysis results strongly coincided with the RNA-seq results ($r^2 = 0.6082$); this finding verified the accuracy of the RNA-seq results (Supplemental Fig. S16, A and B).

Because the above results showed that MHPP significantly induces the expression of glucosinolate biosynthesis-related genes, we evaluated the glucosinolate levels in MHPP-treated plants to determine whether the content of the glucosinolates was altered by MHPP treatment. As

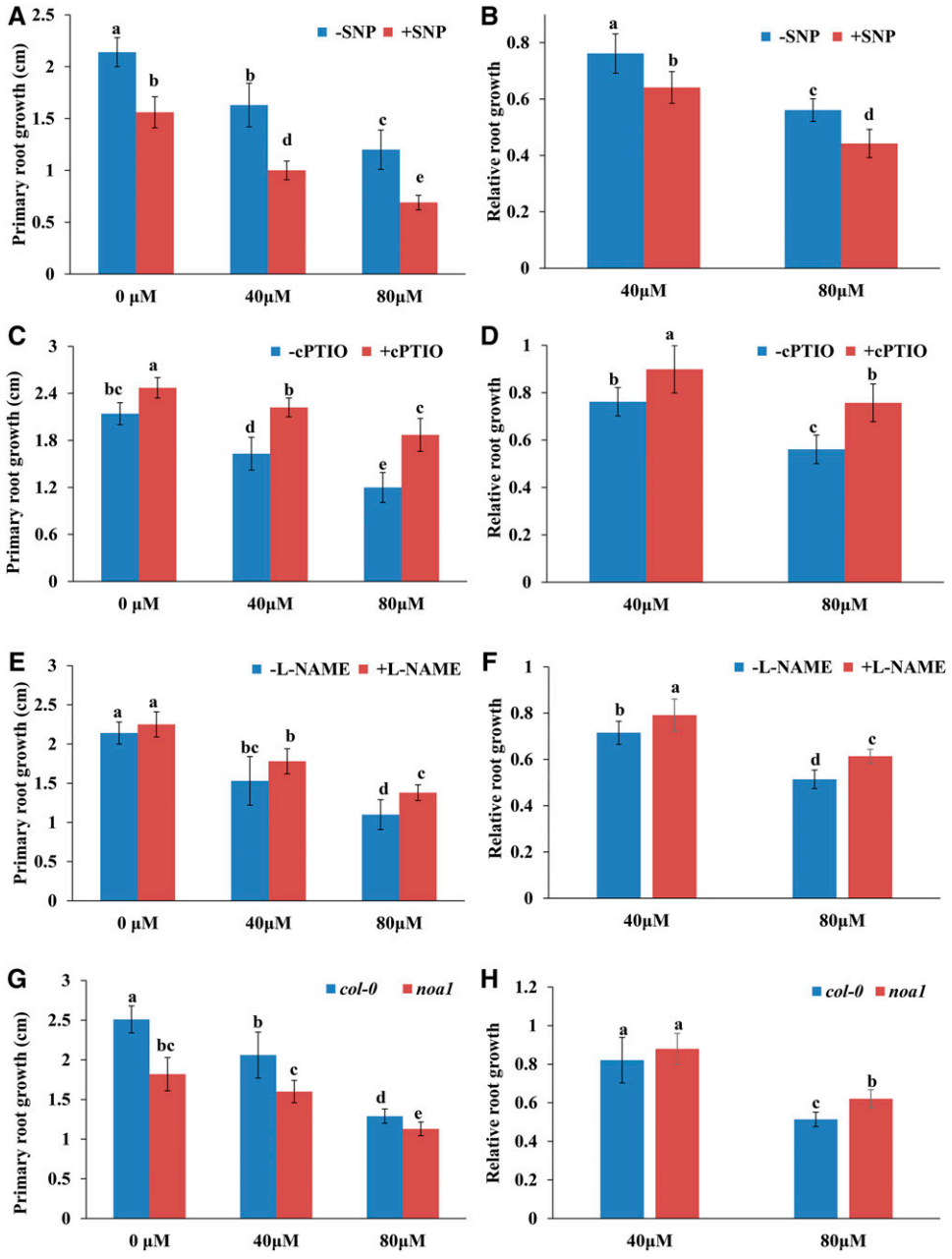

Figure 6. A to F, PR growth of Col-0 seedlings treated with or without MHPP (40 or 80 μM) for 2 d in the presence or absence of 100 μM SNP (A), 200 μM cPTIO (C), or 500 μM L-NAME (E). The data are presented relative to the control values obtained from Col-0 seedlings in the presence or absence of 100 μM SNP (B), 200 μM cPTIO (D), or 500 μM L-NAME (F). G and H, PR growth of Col-0 and *noa1* seedlings treated with or without MHPP (40 or 80 μM) for 2 d (G) and relative root growth of seedlings of the two genotypes treated with 40 or 80 μM MHPP compared with untreated seedlings (H). Error bars represent the SE. Different letters indicate significantly different values ($P < 0.05$ by Tukey's test).

shown in Supplemental Figure S16C, treatment with MHPP significantly induces the accumulation of glucosinolates in roots. Glucosinolates are a group of amino acid-derived metabolites (Shroff et al., 2008). Thus, we examined the contents of free amino acids in MHPP-treated plants. As shown in Supplemental Figure S17, analysis of free amino acid contents revealed a large response to MHPP in Arabidopsis roots. MHPP treatment induced increases in the free amino acid levels in Arabidopsis roots. Among the 17 amino acids evaluated, 13 amino acids, including the precursors of glucosinolate biosynthesis L-Phe, L-Leu, L-Ile, and L-Tyr, displayed higher levels, whereas only two amino acids (Thr and His) displayed lower levels, in the roots of seedlings treated with MHPP compared with untreated control seedlings. Two amino acids (Val and Lys) showed similar concentrations in roots between plants treated with and without MHPP.

Glucosinolates are a class of typical chemical defense molecules in plants, and the glucosinolate biosynthesis pathway is induced by phytohormones such as jasmonic acid (JA) and salicylic acid (SA; van Dam et al., 2004; Tong et al., 2015). Therefore, we next assessed the levels of ABA, JA, and SA in plants in response to MHPP treatment. As shown in Supplemental Figure S18, treatment with MHPP significantly increased the contents of SA and JA by 212% and 627%, respectively, but did not affect the ABA level in the roots of MHPP-treated

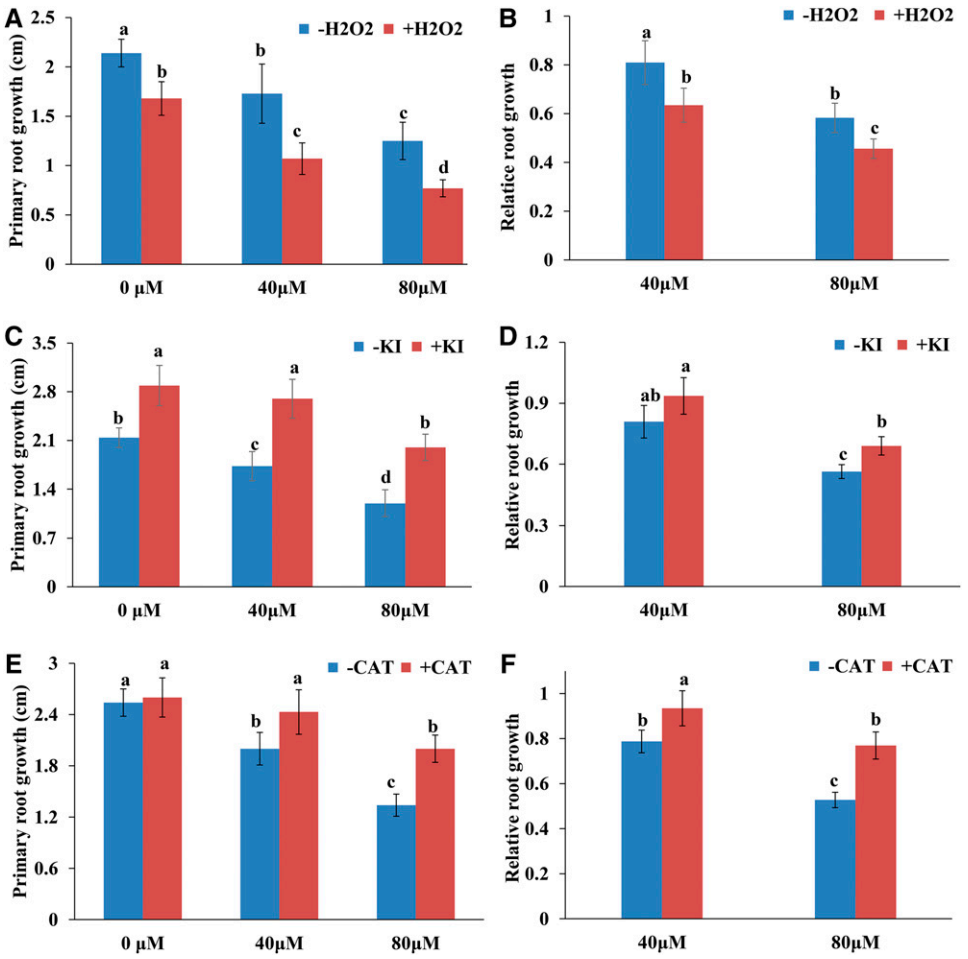

Figure 7. PR growth of Col-0 seedlings treated with or without MHPP (40 or 80 μM) for 2 d in the presence or absence of 500 μM H_2O_2 (A), 1 mM KI (C), or 200 μM CAT (E). The data are presented relative to the control values obtained from Col-0 seedlings in the presence or absence of 500 μM H_2O_2 (B), 1 mM KI (D), or 200 μM CAT (F). Error bars represent the SE. Different letters indicate significantly different values ($P < 0.05$ by Tukey's test).

plants compared with control plants. These data imply that MHPP performs diverse functions in modulating plant growth, development, and defense responses. The detailed molecular mechanisms underlying these functions require further investigation.

DISCUSSION

MHPP Affects Root System Development by Modulating the Levels of Auxin Expression and Signaling

Early reports revealed that the phenolic substance MHPP, an exudate among the specific secondary organic compounds released from roots, possesses strong BNI activity (Subbarao et al., 2013). However, these previous studies focused on the inhibitory effects of MHPP on soil nitrification and nitrogen loss (Nardi et al., 2013), and the effects of MHPP on root system growth and development have not been investigated. Several findings suggest that roots also might be targets of MHPP-mediated plant growth and development: (1) root-secreted secondary metabolites can regulate the growth and development of plants; (2) postembryonic root development is an auxin-driven plastic process that rapidly adapts to external changes; and (3) MHPP treatment enhances nutrient uptake by plants. Here, we show that MHPP inhibits PR growth and promotes LR formation, thus modulating RSA remodeling. We first observed that MHPP inhibits PR elongation and LR formation in a dose-dependent manner. Because the inhibition of root growth is a typical auxin signal phenotype, we hypothesized that MHPP impacts auxin signaling in roots, and we indeed found that MHPP treatment rapidly increased auxin accumulation in root tips.

Our results indicate that MHPP increases the expression of the DR5:GFP reporter in root tips by enhancing auxin biosynthesis, changing PAT, and modulating auxin perception via the destabilization of the Aux/IAA family of transcriptional repressors in root tips. Several lines of evidence support these conclusions. First, GC-MS analysis confirmed elevated IAA contents in MHPP-treated plants, and at the molecular level, auxin biosynthesis-related genes were markedly up-regulated after MHPP treatment. Second, MHPP markedly affected the expression levels of PIN4, and genetic analysis supported the hypothesis that MHPP mediates auxin accumulation in root tips by affecting PAT via the modulation of PIN4. Third, the MHPP-mediated rapid degradation of Aux/IAA proteins was

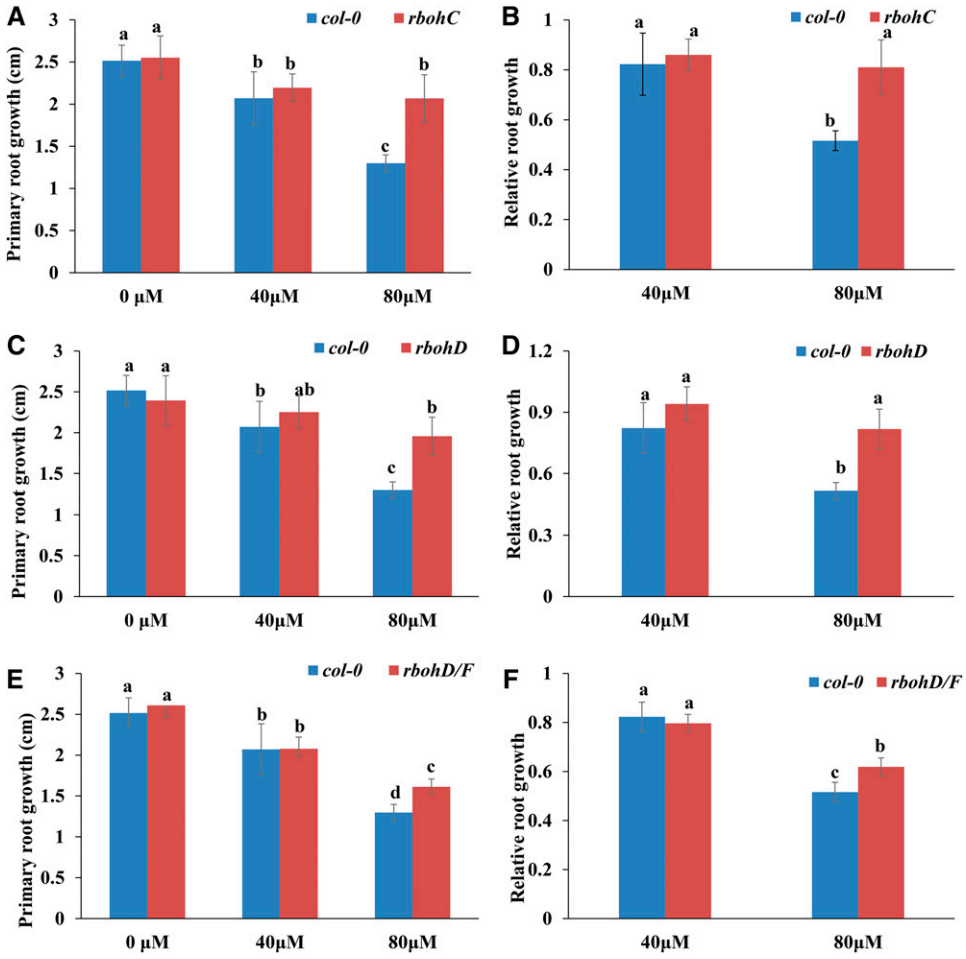

Figure 8. A and B, PR growth of Col-0 and *rbohC* seedlings treated with or without MHPP (40 or 80 μM) for 2 d (A) and relative root growth of the two genotypes treated with 40 or 80 μM MHPP compared with untreated seedlings (B). C and D, PR growth of Col-0 and *rbohD* seedlings treated with or without MHPP (40 or 80 μM) for 2 d (C) and relative root growth of seedlings of the two genotypes treated with 40 or 80 μM MHPP compared with untreated seedlings (D). E and F, PR growth of Col-0 and *rbohD/F* seedlings treated with or without MHPP (40 or 80 μM) for 2 d (E) and relative root growth of seedlings of the two genotypes treated with 40 or 80 μM MHPP compared with untreated seedlings (F). Error bars represent the SE. Different letters indicate significantly different values ($P < 0.05$ by Tukey's test).

confirmed by examining DII-VENUS marker fluorescence and the GUS staining of *HS:AXR3-GUS* plants. Fourth, physiologically, exogenous application of IAA enhanced the inhibitory effects of MHPP on PR growth, and genetic analysis supported this result in the auxin-overproducing mutant *yucca* and the auxin-insensitive mutant *axr3-3*.

Proper auxin accumulation relies on the coordination between its biosynthesis and transport (Liu et al., 2015). Treatment with the auxin transport inhibitor NPA or mutation of the *PIN* family of auxin carrier genes affects root growth (Blilou et al., 2005; Liu et al., 2015), and these observations suggest that disturbing PAT changes auxin accumulation in root tips and subsequently alters root growth. In this study, we found that NPA did not affect the MHPP-mediated inhibitory effects on PR elongation; this finding suggests that PAT is involved in MHPP-mediated root growth inhibition. Investigation of the expression levels of auxin carriers showed that MHPP significantly modulated the expression of PIN4. Furthermore, the *pin4-3* mutant exhibited reduced sensitivity to MHPP treatment in terms of PR growth, suggesting that PIN4 at least partly mediates MHPP-induced auxin accumulation to inhibit PR growth. PIN4 regulates auxin levels and gradients in the root meristem, and *pin4* mutant seedlings accumulate higher auxin levels in root tips (Friml et al., 2002). Our results indicated that MHPP treatment markedly reduced PIN4 expression and thereby disrupted auxin transport, leading to auxin accumulation in root tips. However, how PIN4 is involved in the MHPP-mediated modulation of PR growth remains to be explored.

Changes in Aux/IAA stability and, subsequently, the auxin perception level appear to represent a general strategy by which plants interplay with phytohormones and respond to environmental cues (Yuan et al., 2013; Bailly et al., 2014; Katz et al., 2015; Li et al., 2015; Liu et al., 2015; Yuan and Huang, 2016). Treatment with SA reduces auxin responses by stabilizing Aux/IAA proteins (Wang et al., 2007). Gain-of-function mutations of Aux/IAA proteins such as *IAA3* and *IAA17* induce defective root development (Hamann et al., 2002; Liu et al., 2015). We found that MHPP treatment enhanced the degradation of Aux/IAA proteins, as revealed by GUS staining of the *HS:AXR3-GUS* reporter line, and thereby amplified auxin signaling in root tips. We also observed reduced sensitivity of the *axr3-3* mutant to MHPP treatment compared with the wild-type control in terms of PR growth. MHPP treatment might not induce the degradation of mutant AXR3 in *axr3-3*,

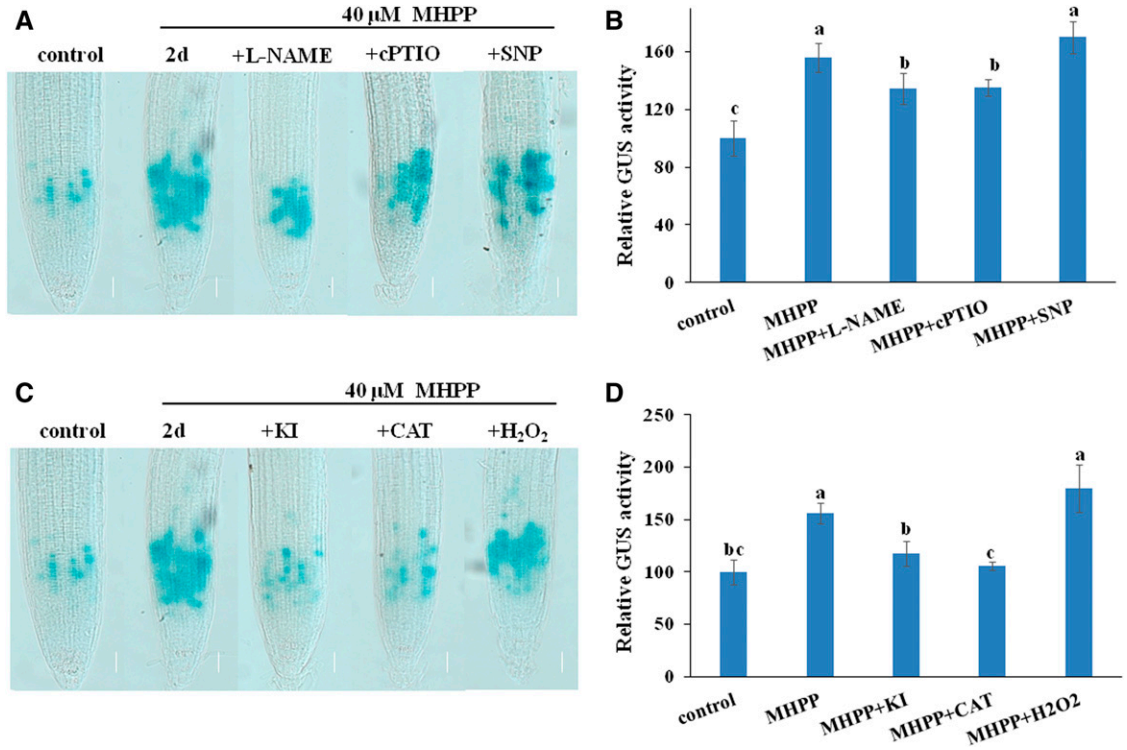

Figure 9. NO and ROS are involved in the MHPP-mediated reduction of meristematic cell division potential. A and B, GUS staining of 5-d-old *CYCB1;1:GUS* seedlings exposed to 40 μM MHPP for 2 d in the presence or absence of 500 μM L-NAME, 200 μM cPTIO, or 100 μM SNP (A) and relative GUS activity of *CYCB1;1:GUS* seedlings (B) treated as in A. C and D, GUS staining of 5-d-old *CYCB1;1:GUS* seedlings exposed to 40 μM MHPP for 2 d in the presence or absence of 1 mM KI, 200 μM CAT, or 500 μM H_2O_2 (C) and relative GUS activity of *CYCB1;1:GUS* seedlings (D) treated as in C. The level of GUS activity in untreated roots was set to 100. Error bars represent the SE. Different letters indicate significantly different values ($P < 0.05$ by Tukey's test). Bars = 50 μm.

preventing MHPP from altering auxin signaling and subsequently inhibiting PR growth. Taken together, the results presented here clearly demonstrate that MHPP influences root growth by modulating the levels of auxin expression and signaling.

MHPP Affects Meristematic Cell Division Potential in Root Tips

Root growth is maintained by coordinating cell proliferation and differentiation. Root tissue cells are derived from the stem cell niche, which is composed of an inner group of mitotically inactive QC cells and an outer group of mitotically active stem cells (Dinneny and Benfey, 2008; Ji et al., 2015). Root stem cell niche activity and meristematic cell division potential are two crucial determinants of root meristem size and root growth (Aida et al., 2004; Della Rovere et al., 2013; Ji et al., 2015). In this study, we found that MHPP treatment did not change the expression levels of the QC marker QC25:GUS. Both the *SHR/SCARECROW* (*SCR*) pathway and the *PLT* pathway regulate QC identity and stem cell niche activity. *SHR* is expressed primarily in the stele, and the encoded protein can move to the QC and other surrounding cells to activate the expression of *SCR* together with *WOX5* to coordinately regulate QC identity and the balance between root stem cell division and differentiation. The *PLT* pathway modulates the auxin-dependent maintenance of the stem cell niche (Aida et al., 2004; Galinha et al., 2007). Neither SHR nor PLT1 protein was altered in MHPP-treated plants, and our finding suggests that MHPP treatment does not affect QC cell-specific expression or root apical meristem activity. Thus, we examined whether MHPP affects meristematic cell division potential. Our results from GUS staining of the *CYCB1;1:GUS* reporter line revealed that the percentage of GUS-stained cells in the root meristem was significantly greater in MHPP-treated roots than in control roots. These results imply that treatment with MHPP decelerated the cell cycle. These data indicate that MHPP treatment inhibits PR growth by affecting meristematic cell division potential but not stem cell niche activity.

NO-Mediated ROS Accumulation in Root Tips Modifies the RSA in Response to MHPP Treatment via the Auxin Pathway

In this study, we obtained evidence for the involvement of ROS in NO signaling during the response of

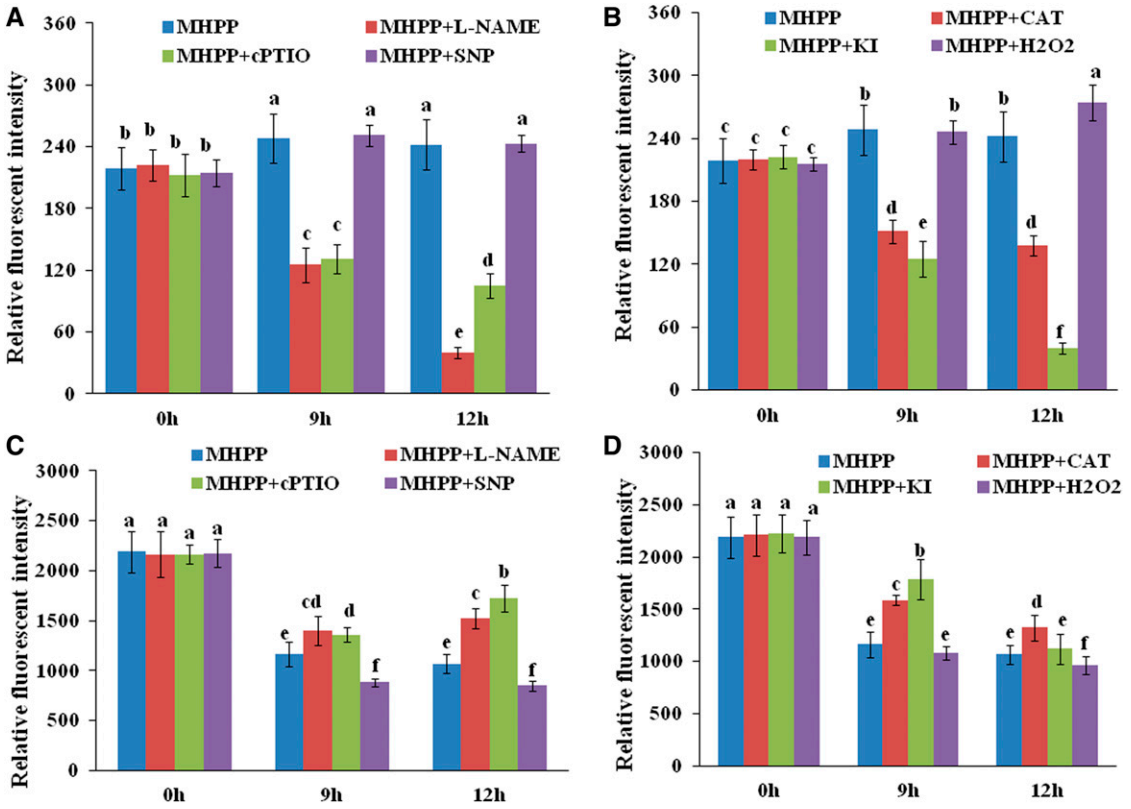

Figure 10. NO and ROS are involved in the MHPP-mediated accumulation of auxin in root tips and the inhibition of root meristem development. Quantification of the DR5:GFP fluorescence intensity (A and B) and DII-VENUS fluorescence intensity (C and D) is shown in the roots of *DR5:GFP* (A and B) or *DII-VENUS* (C and D) seedlings treated with or without 40 μM MHPP in the presence or absence of 500 μM L-NAME, 200 μM cPTIO, 100 μM SNP, 200 μM CAT, 1 mM KI, or 500 μM H_2O_2 for 9 or 12 h. For representative images, see Supplemental Figures S9 to S12.

plants to MHPP treatment. We found that treatment with MHPP induced the accumulation of NO and ROS in roots. Supplementation with the NO scavenger cPTIO or the NO synthase inhibitor L-NAME markedly inhibited ROS accumulation, and this effect also was observed in the *noa1* mutant. In contrast, supplementation with the ROS scavenger KI did not affect NO production in MHPP-treated roots. These results suggest that NO acts upstream of ROS in the response of plant roots to MHPP treatment. Pharmacological analysis using NO/ROS scavengers and genetic analysis using NO-/ROS-related mutants indicated that NO/ROS accumulation contributes to MHPP-mediated PR growth inhibition. Further investigation using the *CYCB1;1:GUS* reporter indicated that NO and ROS mediate the MHPP-induced inhibition of PR growth by reducing meristematic cell division potential.

Previous studies revealed that disrupting NO production reduced DR5:GUS expression in roots (Sanz et al., 2014). NO also affected auxin signaling by promoting the degradation of IAA17 (Terrile et al., 2012). In agreement with these findings, our study indicated that inhibition of NO production reduced the expression of the auxin-responsive reporter *DR5:GFP* but stabilized DII-VENUS marker fluorescence in MHPP-treated roots. Interestingly, Liu et al. (2015) found that NO reduced auxin responses and increased the stability of IAA17 in roots subjected to salt stress. The difference in these effects between studies may be due to the distinct stresses and environmental cues examined, as auxin responses and NO functions differ according to the type of stress or tissue.

ROS is another important signaling molecule that plays an important role in plant growth and environmental responses (Tsukagoshi et al., 2010). ROS regulates the balance between cellular proliferation and differentiation in roots (Tsukagoshi et al., 2010). It has been reported that the ROS and auxin pathways can impact each other extensively (Kwak et al., 2006). Interestingly, Blomster et al. (2011) found that ozone, an apoplastic form of ROS, transiently suppresses auxin signaling by reducing the gene expression of auxin receptors and the Aux/IAA family of transcriptional repressors. In this study, inhibiting H_2O_2 production reduced the expression of the auxin-responsive *DR5:GFP* reporter but stabilized DII-VENUS marker fluorescence in MHPP-treated roots, and our findings suggest that ROS contributes to the MHPP-mediated alterations in the levels of auxin expression and signaling in roots. The differences in these effects of ROS

on auxin signaling between studies may be due to the distinct forms of ROS examined, as the response of plants to ROS varies depending on the form of ROS. Furthermore, these studies of the function of ROS in the plant response to environmental cues were based on the use of exogenous ROS donors. However, environmental cues, such as stresses, might induce endogenous ROS production; therefore, ROS might play specific roles in response to certain cues. In conclusion, our results indicate that MHPP treatment inhibits PR growth by increasing NO and ROS levels. The elevated accumulation of NO and ROS further altered the levels of auxin expression and perception to amplify auxin signaling.

The MHPP-Induced Accumulation of Plant Defense Molecules Implies Its Diverse Functions in Modulating Plant Growth, Development, and Stress Tolerance

Glucosinolates, a group of sulfur-rich, amino acid-derived metabolites, are among the most extensively studied classes of antiherbivore defense chemicals in plants. Upon insect feeding or mechanical damage, glucosinolates are hydrolyzed into aglycone by myrosinase and subsequently form isothiocyanates, nitriles, and other products (Bones and Rossiter, 2006). These natural chemicals, which most likely contribute to plant defense against pests and diseases, also are detected in small amounts in humans and are believed to contribute to the health-promoting properties of cruciferous vegetables (Halkier and Gershenzon, 2006; Shroff et al., 2008). Interestingly, MHPP treatment induced the accumulation of glucosinolates and their amino acid precursors in roots. We also observed significantly elevated levels of two defense signaling phytohormones, SA and JA, in MHPP-treated plants. These data suggest that MHPP induces the production of plant defense-related metabolites and that MHPP might promote antiherbivore defense responses in plants. Further studies will focus on how MHPP elevates the levels of JA and SA and whether the MHPP-induced accumulation of JA and SA is involved in the enhancement of glucosinolate production in plants.

In this study, we also found that MHPP treatment promoted LR development. LR formation is tightly mediated by the auxin pathway (Li et al., 2015). The induction of the expression of IAA biosynthesis-related genes in seedlings and the increase in the IAA content in roots might partly explain the enhancement of LR development in response to MHPP treatment. However, the detailed molecular mechanisms involved in MHPP-induced LR formation and whether the changes in the expression of PIN4 also are involved in MHPP-induced LR development remain to be explored further. Increased LR formation altered the RSA, ultimately benefiting the uptake of water and nutrient elements into roots. Indeed, we found that MHPP markedly increased the contents of nutrient elements in seedlings, including P, K, S, Fe, Mn, Zn, and Cu. This observation indicated that MHPP enhanced nutrient element accumulation in plants. Further studies will examine whether MHPP could regulate the expression of the transporters of nutrient elements and metal ions in plants and affect the transport of nutrient elements from the roots to aboveground portions of plants.

In conclusion, our data indicate that MHPP, in addition to its function as a nitrification inhibitor, profoundly impacts root development. Based on our results, MHPP inhibits PR elongation by regulating the levels of auxin expression, transport, and signaling in roots and consequently altering root meristematic cell division potential, and the NO/ROS pathway is involved in these processes. Moreover, treatment with MHPP increases nutrient element uptake and plant defense-related metabolite accumulation in roots. Although the possible involvement of other pathways in MHPP-induced RSA remodeling remains to be explored, our findings show that MHPP modulates plant growth, development, and stress tolerance by inducing morphological and physiological changes in roots. Further research examining the interplay of MHPP with phytohormones will enable a broader understanding of the mechanism by which plants respond to MHPP by regulating hormonal signaling, will aid in the development of cost-effective, sustainable agricultural strategies for crop breeding and cultivation, and will provide insight into novel applications of this biological nitrification inhibitor.

MATERIALS AND METHODS

Plant Growth and Chemical Treatments

Arabidopsis (*Arabidopsis thaliana*) seedlings of the following lines were used in this study: Col-0; the mutants *yucca*, *pin4-3*, *axr3-3*, *axr1-12*, *noa1*, *rbohC*, *rbohD*, *rbohD/F*, *pin1*, *pin2*, *pin7-2*, and *aux1-21* in the Col-0 background; and the transgenic lines *DR5:GFP*, *PIN1:PIN1-GFP*, *PIN2:PIN2-GFP*, *PIN4:PIN4-GFP*, *PIN7:PIN7-GFP*, *AUX1:AUX1-YFP*, *PLT1:PLT1-GFP*, *SHR:SHR-GFP*, *DII-VENUS*, *mDII-VENUS*, *QC25:GUS*, *CYCB1;1:GUS*, *HS:AXR3NT-GUS*, and *HS:GUS*.

Seeds were surface sterilized and plated on agar medium containing one-half-strength MS medium (Sigma-Aldrich), pH 5.75, supplemented with 1% agar and 10% Suc. Seedlings were grown in a vertical position in a growth chamber maintained at 22°C under a 16/8-h light/dark cycle. Five-day-old seedlings were transferred to plates supplemented with various chemicals, such as MHPP, IAA, NPA, SNP, cPTIO, and L-NAME, and grown for an additional 2 to 5 d. All chemicals were obtained from Sigma-Aldrich.

GUS Staining

To detect the expression of GUS, we incubated *QC25:GUS* or *CYCB1;1:GUS* seedlings in GUS buffer containing the substrate 1 mM 5-bromo-4-chloro-3-indolyl-β-D-GlcA cyclohexyl-ammonium (Sigma-Aldrich) at 37°C in the dark (Ulmasov et al., 1997). The GUS staining duration was dependent on the transgenic marker line: 5 h for *QC25:GUS* and 3 h for *CYCB1;1:GUS*. MUG assays were performed according to a previously described method (Côté and Rutledge, 2003). The seedlings were washed and placed in 75% (w/v) ethanol before examination with a microscope (Zeiss Axioskop). At least 20 seedlings were analyzed for each treatment. The experiments were repeated at least three times.

Measurement of the Production of NO and H_2O_2

Endogenous NO levels in root meristems were visualized using the NO-specific fluorescent probe DAF-2 DA (Beyotime). Seedlings were incubated at 37°C in 5 μM staining solution for 1 h. Then, the samples were washed twice and

viewed with a Leica laser scanning confocal microscope (excitation, 490 nm; emission, 515 nm). Quantitative measurement of fluorescence intensity was performed using ImageJ.

Endogenous H_2O_2 levels in root meristems were visualized using the H_2O_2-specific fluorescent probe DCFH-DA (Beyotime). Seedlings were incubated at 37°C in 10 μM staining solution for 5 min. Then, the samples were washed twice and viewed with a Leica laser scanning confocal microscope (excitation, 488 nm; emission, 530 nm). Quantitative measurement of fluorescence intensity was performed using ImageJ.

Phenotypic Analysis

Relative root growth was calculated as the length of root growth under the treatment conditions divided by the mean root length under control conditions as described by Freeman et al. (2010). At least 15 replicate plants were measured for each treatment. Measurements of the lengths of meristem zones and elongation zones and the average cell length in the differentiation zone were performed according to published methods (Dello Ioio et al., 2007; Yuan et al., 2013; Liu et al., 2015). LRP initiation was quantified in roots using the *DR5:GUS* reporter line. The four developmental stages of the LRP were classified as follows: up to three cell layers (stage A); more than three cell layers but nonemerged (stage B); emerged LRs less than 0.5 mm in length (stage C); and emerged LRs greater than 0.5 mm in length (stage D; Zhang et al., 1999; Li et al., 2015). Only mature LRs (greater than 0.5 mm) are denoted as LRs.

qRT-PCR Analysis

Seedlings were collected for total RNA isolation using TRIzol Reagent (TaKaRa) according to the manufacturer's instructions. The RNA concentration was accurately quantified using spectrophotometry. Then, complementary DNA (cDNA) was synthesized from DNase-treated total RNA (1 μg) using a Reverse Transcription System Kit (Promega) and oligo(dT) primers. The cDNA produced was diluted 1:15, and 3 μL of diluted cDNA was employed for qRT-PCR in a 7500 Real Time System (Applied Biosystems) using Platinum SYBR Green qPCR SuperMix-UDG (Invitrogen). *ACTIN2* (AT3G18780) and *EF1a* (AT5G60390) were used as internal controls for qRT-PCR normalization using GeNorm (Czechowski et al., 2005). For each gene, qRT-PCR was performed on three biological replicates, with duplicates for each biological replicate. The relative transcript level was determined for each sample and was averaged over the six replicates. The specific primers used for each gene are listed in Supplemental Table S2. All primer pairs produced only one peak in DNA melting curves, and this result indicated the high specificity of the primers.

Quantification of IAA Content

IAA content was quantified according to Gao et al. (2014) and Liu et al. (2015). Root tips of approximately 0.1 g fresh weight were collected and immediately frozen in liquid nitrogen. After extraction, endogenous IAAs were purified, methylated in a stream of diazomethane gas, and resuspended in 100 μL of ethyl acetate. The endogenous IAA content was analyzed by GC-MS.

Nutrient Element Content Analysis

Seedlings grown in one-half-strength MS medium were treated with 40 μM MHPP for 2 d. The treated roots were immersed in a solution containing 1 mM EDTA for 2 h and then rinsed thoroughly with distilled water. The dried plant tissues were ground and digested in concentrated nitric acid for 2 d at room temperature. Next, the samples were boiled for 2 h until completely digested. After adding 3 mL of Millipore-filtered deionized water and brief centrifugation, the contents of Zn, Fe, Mn, and Cu were determined using inductively coupled plasma-mass spectrometry, and the contents of P, K, and S were determined using inductively coupled plasma-atomic emission spectroscopy. Each experiment was repeated three times.

Statistical Analysis

For each treatment, at least 12 roots were analyzed; all experiments were repeated at least three times. The results are presented as means ± SE. For statistical analysis, we used Tukey's test ($P < 0.01$).

Supplemental Data

The following supplemental materials are available.

Supplemental Figure S1. Effects of MHPP on root meristem development.

Supplemental Figure S2. GFP fluorescence in the roots of *DR5:GFP* or *PIN4:GFP* seedlings.

Supplemental Figure S3. GFP/YFP fluorescence in the roots of *PIN1/2/7:GFP* and *AUX1:YFP* seedlings.

Supplemental Figure S4. Relative root growth of seedlings exposed to MHPP.

Supplemental Figure S5. YFP fluorescence in the roots of *DII-VENUS* or *mDII-VENUS* seedlings.

Supplemental Figure S6. Detection of NO and H_2O_2 production.

Supplemental Figure S7. ROS and NO in the roots of wild-type seedlings in response to MHPP.

Supplemental Figure S8. Image of DAB staining.

Supplemental Figure S9. GFP fluorescence in the roots of *DR5:GFP* seedlings (1).

Supplemental Figure S10. GFP fluorescence in the roots of *DR5:GFP* seedlings (2).

Supplemental Figure S11. YFP fluorescence in the roots of *DII-VENUS* seedlings (1).

Supplemental Figure S12. YFP fluorescence in the roots of *DII-VENUS* seedlings (2).

Supplemental Figure S13. Hierarchical clustering analysis.

Supplemental Figure S14. Kyoto Encyclopedia of Genes and Genomes pathway enrichment analysis.

Supplemental Figure S15. Modulation of glucosinolate biosynthesis after MHPP treatment.

Supplemental Figure S16. MHPP up-regulates several genes involved in glucosinolate biosynthesis.

Supplemental Figure S17. MHPP affects the free amino acid contents.

Supplemental Figure S18. Contents of ABA, SA, and JA.

Supplemental Table S1. Differential expression of genes involved in glucosinolate biosynthesis.

Supplemental Table S2. List of primers for qRT-PCR analysis of the genes.

Supplemental Materials and Methods. Supplemental Materials and Methods to accompany this article.

ACKNOWLEDGMENTS

We thank Shaojian Zheng (Zhejiang University) for providing *yucca* seeds, Yingtang Lu (Wuhan University) and Dr. Hongmei Yuan (Hainan University) for providing *pin1* seeds, the Arabidopsis Biological Resource Center for the mutant seeds, Zhaojun Ding (Shandong University) for helpful discussion and guidance, and the Central Laboratory of the Xishuangbanna Tropical Botanical Garden for providing research facilities.

Received April 29, 2016; accepted May 18, 2016; published May 23, 2016.

LITERATURE CITED

Aida M, Beis D, Heidstra R, Willemsen V, Blilou I, Galinha C, Nussaume L, Noh YS, Amasino R, Scheres B (2004) The PLETHORA genes mediate patterning of the Arabidopsis root stem cell niche. Cell **119:** 109–120

Bailly A, Groenhagen U, Schulz S, Geisler M, Eberl L, Weisskopf L (2014) The inter-kingdom volatile signal indole promotes root development by interfering with auxin signalling. Plant J **80:** 758–771

Baluska F, Mancuso S, Volkmann D, Barlow PW (2010) Root apex transition zone: a signalling-response nexus in the root. Trends Plant Sci **15:** 402–408

Bashandy T, Guilleminot J, Vernoux T, Caparros-Ruiz D, Ljung K, Meyer Y, Reichheld JP (2010) Interplay between the NADP-linked thioredoxin and glutathione systems in *Arabidopsis* auxin signaling. Plant Cell **22:** 376–391

Blilou I, Xu J, Wildwater M, Willemsen V, Paponov I, Friml J, Heidstra R, Aida M, Palme K, Scheres B (2005) The PIN auxin efflux facilitator network controls growth and patterning in Arabidopsis roots. Nature **433:** 39–44

Blomster T, Salojärvi J, Sipari N, Brosché M, Ahlfors R, Keinänen M, Overmyer K, Kangasjärvi J (2011) Apoplastic reactive oxygen species transiently decrease auxin signaling and cause stress-induced morphogenic response in Arabidopsis. Plant Physiol **157:** 1866–1883

Bones AM, Rossiter JT (2006) The enzymic and chemically induced decomposition of glucosinolates. Phytochemistry **67:** 1053–1067

Brunoud G, Wells DM, Oliva M, Larrieu A, Mirabet V, Burrow AH, Beeckman T, Kepinski S, Traas J, Bennett MJ, et al (2012) A novel sensor to map auxin response and distribution at high spatio-temporal resolution. Nature **482:** 103–106

Colón-Carmona A, You R, Haimovitch-Gal T, Doerner P (1999) Spatio-temporal analysis of mitotic activity with a labile cyclin-GUS fusion protein. Plant J **20:** 503–508

Correa-Aragunde N, Graziano M, Lamattina L (2004) Nitric oxide plays a central role in determining lateral root development in tomato. Planta **218:** 900–905

Côté C, Rutledge RG (2003) An improved MUG fluorescent assay for the determination of GUS activity within transgenic tissue of woody plants. Plant Cell Rep **21:** 619–624

Czechowski T, Stitt M, Altmann T, Udvardi MK, Scheible WR (2005) Genome-wide identification and testing of superior reference genes for transcript normalization in Arabidopsis. Plant Physiol **139:** 5–17

Della Rovere F, Fattorini L, D'Angeli S, Veloccia A, Falasca G, Altamura MM (2013) Auxin and cytokinin control formation of the quiescent centre in the adventitious root apex of Arabidopsis. Ann Bot (Lond) **112:** 1395–1407

Dello Ioio R, Linhares FS, Scacchi E, Casamitjana-Martinez E, Heidstra R, Costantino P, Sabatini S (2007) Cytokinins determine Arabidopsis root-meristem size by controlling cell differentiation. Curr Biol **17:** 678–682

Dinneny JR, Benfey PN (2008) Plant stem cell niches: standing the test of time. Cell **132:** 553–557

Fan SC, Lin CS, Hsu PK, Lin SH, Tsay YF (2009) The *Arabidopsis* nitrate transporter NRT1.7, expressed in phloem, is responsible for source-to-sink remobilization of nitrate. Plant Cell **21:** 2750–2761

Fernández-Marcos M, Sanz L, Lewis DR, Muday GK, Lorenzo O (2011) Nitric oxide causes root apical meristem defects and growth inhibition while reducing PIN-FORMED 1 (PIN1)-dependent acropetal auxin transport. Proc Natl Acad Sci USA **108:** 18506–18511

Freeman JL, Tamaoki M, Stushnoff C, Quinn CF, Cappa JJ, Devonshire J, Fakra SC, Marcus MA, McGrath SP, Van Hoewyk D, et al (2010) Molecular mechanisms of selenium tolerance and hyperaccumulation in *Stanleya pinnata*. Plant Physiol **153:** 1630–1652

Friml J, Benková E, Blilou I, Wisniewska J, Hamann T, Ljung K, Woody S, Sandberg G, Scheres B, Jürgens G, et al (2002) AtPIN4 mediates sink-driven auxin gradients and root patterning in *Arabidopsis*. Cell **108:** 661–673

Galinha C, Hofhuis H, Luijten M, Willemsen V, Blilou I, Heidstra R, Scheres B (2007) PLETHORA proteins as dose-dependent master regulators of *Arabidopsis* root development. Nature **449:** 1053–1057

Gao X, Yuan HM, Hu YQ, Li J, Lu YT (2014) Mutation of Arabidopsis CATALASE2 results in hyponastic leaves by changes of auxin levels. Plant Cell Environ **37:** 175–188

Gray WM, Kepinski S, Rouse D, Leyser O, Estelle M (2001) Auxin regulates SCF(TIR1)-dependent degradation of AUX/IAA proteins. Nature **414:** 271–276

Halkier BA, Gershenzon J (2006) Biology and biochemistry of glucosinolates. Annu Rev Plant Biol **57:** 303–333

Hamann T, Benkova E, Bäurle I, Kientz M, Jürgens G (2002) The Arabidopsis BODENLOS gene encodes an auxin response protein inhibiting MONOPTEROS-mediated embryo patterning. Genes Dev **16:** 1610–1615

Iglesias MJ, Terrile MC, Bartoli CG, D'Ippólito S, Casalongué CA (2010) Auxin signaling participates in the adaptative response against oxidative stress and salinity by interacting with redox metabolism in Arabidopsis. Plant Mol Biol **74:** 215–222

Ji H, Wang S, Li K, Szakonyi D, Koncz C, Li X (2015) PRL1 modulates root stem cell niche activity and meristem size through WOX5 and PLTs in Arabidopsis. Plant J **81:** 399–412

Katz E, Nisani S, Yadav BS, Woldemariam MG, Shai B, Obolski U, Ehrlich M, Shani E, Jander G, Chamovitz DA (2015) The glucosinolate breakdown product indole-3-carbinol acts as an auxin antagonist in roots of Arabidopsis thaliana. Plant J **82:** 547–555

Kovtun Y, Chiu WL, Tena G, Sheen J (2000) Functional analysis of oxidative stress-activated mitogen-activated protein kinase cascade in plants. Proc Natl Acad Sci USA **97:** 2940–2945

Kwak JM, Nguyen V, Schroeder JI (2006) The role of reactive oxygen species in hormonal responses. Plant Physiol **141:** 323–329

Laskowski M, Grieneisen VA, Hofhuis H, Hove CA, Hogeweg P, Marée AFM, Scheres B (2008) Root system architecture from coupling cell shape to auxin transport. PLoS Biol **6:** e307

Li J, Xu HH, Liu WC, Zhang XW, Lu YT (2015) Ethylene inhibits root elongation during alkaline stress through AUXIN1 and associated changes in auxin accumulation. Plant Physiol **168:** 1777–1791

Liu W, Li RJ, Han TT, Cai W, Fu ZW, Lu YT (2015) Salt stress reduces root meristem size by nitric oxide-mediated modulation of auxin accumulation and signaling in Arabidopsis. Plant Physiol **168:** 343–356

Lombardo MC, Graziano M, Polacco JC, Lamattina L (2006) Nitric oxide functions as a positive regulator of root hair development. Plant Signal Behav **1:** 28–33

Nardi P, Akutsu M, Pariasca-Tanaka J, Wissuwa M (2013) Effect of methyl 3-4-hydroxyphenyl propionate, a Sorghum root exudate, on N dynamic, potential nitrification activity and abundance of ammonia-oxidizing bacteria and archaea. Plant Soil **367:** 627–637

Oono Y, Ooura C, Rahman A, Aspuria ET, Hayashi K, Tanaka A, Uchimiya H (2003) p-Chlorophenoxyisobutyric acid impairs auxin response in Arabidopsis root. Plant Physiol **133:** 1135–1147

Overvoorde P, Fukaki H, Beeckman T (2010) Auxin control of root development. Cold Spring Harb Perspect Biol **2:** a001537

Péret B, Swarup K, Ferguson A, Seth M, Yang Y, Dhondt S, James N, Casimiro I, Perry P, Syed A, et al (2012) AUX/LAX genes encode a family of auxin influx transporters that perform distinct functions during *Arabidopsis* development. Plant Cell **24:** 2874–2885

Rouse D, Mackay P, Stirnberg P, Estelle M, Leyser O (1998) Changes in auxin response from mutations in an AUX/IAA gene. Science **279:** 1371–1373

Sabatini S, Beis D, Wolkenfelt H, Murfett J, Guilfoyle T, Malamy J, Benfey P, Leyser O, Bechtold N, Weisbeek P, et al (1999) An auxin-dependent distal organizer of pattern and polarity in the Arabidopsis root. Cell **99:** 463–472

Sanz L, Fernández-Marcos M, Modrego A, Lewis DR, Muday GK, Pollmann S, Dueñas M, Santos-Buelga C, Lorenzo O (2014) Nitric oxide plays a role in stem cell niche homeostasis through its interaction with auxin. Plant Physiol **166:** 1972–1984

Schlesinger WH (2009) On the fate of anthropogenic nitrogen. Proc Natl Acad Sci USA **106:** 203–208

Shroff R, Vergara F, Muck A, Svatos A, Gershenzon J (2008) Nonuniform distribution of glucosinolates in Arabidopsis thaliana leaves has important consequences for plant defense. Proc Natl Acad Sci USA **105:** 6196–6201

Subbarao GV, Nakahara K, Ishikawa T, Ono H, Yoshida M, Yoshihashi T, Zhu YY, Zakir HAKM, Deshpande SP, Hash CT, et al (2013) Biological nitrification inhibition (BNI) activity in sorghum and its characterization. Plant Soil **366:** 243–259

Terrile MC, París R, Calderón-Villalobos LIA, Iglesias MJ, Lamattina L, Estelle M, Casalongué CA (2012) Nitric oxide influences auxin signaling through S-nitrosylation of the Arabidopsis TRANSPORT INHIBITOR RESPONSE 1 auxin receptor. Plant J **70:** 492–500

Tewari RK, Kim S, Hahn EJ, Paek KY (2008) Involvement of nitric oxide-induced NADPH oxidase in adventitious root growth and antioxidant defense in Panax ginseng. Plant Biotechnol Rep **2:** 113–122

Tong Y, Gabriel-Neumann E, Krumbein A, Ngwene B, George E, Schreiner M (2015) Interactive effects of arbuscular mycorrhizal fungi and intercropping with sesame (Sesamum indicum) on the glucosinolate profile in broccoli (Brassica oleracea var. italica). Environ Exp Bot **109:** 288–295

Tsukagoshi H, Busch W, Benfey PN (2010) Transcriptional regulation of ROS controls transition from proliferation to differentiation in the root. Cell **143:** 606–616

Ulmasov T, Murfett J, Hagen G, Guilfoyle TJ (1997) Aux/IAA proteins repress expression of reporter genes containing natural and highly active synthetic auxin response elements. Plant Cell **9:** 1963–1971

van Dam NM, Witjes L, Svatos A (2004) Interactions between aboveground and belowground induction of glucosinolates in two wild Brassica species. New Phytol **161:** 801–810

Van de Poel B, Smet D, Van Der Straeten D (2015) Ethylene and hormonal cross talk in vegetative growth and development. Plant Physiol **169:** 61–72

Wang D, Pajerowska-Mukhtar K, Culler AH, Dong X (2007) Salicylic acid inhibits pathogen growth in plants through repression of the auxin signaling pathway. Curr Biol **17:** 1784–1790

Wang Y, Li K, Li X (2009) Auxin redistribution modulates plastic development of root system architecture under salt stress in Arabidopsis thaliana. J Plant Physiol **166:** 1637–1645

Wink DA, Mitchell JB (1998) Chemical biology of nitric oxide: insights into regulatory, cytotoxic, and cytoprotective mechanisms of nitric oxide. Free Radic Biol Med **25:** 434–456

Xu J, Yin H, Li Y, Liu X (2010a) Nitric oxide is associated with long-term zinc tolerance in *Solanum nigrum*. Plant Physiol **154:** 1319–1334

Xu J, Yin H, Liu X, Li X (2010b) Salt affects plant Cd-stress responses by modulating growth and Cd accumulation. Planta **231:** 449–459

Xu J, Zhu Y, Ge Q, Li Y, Sun J, Zhang Y, Liu X (2012) Comparative physiological responses of Solanum nigrum and Solanum torvum to cadmium stress. New Phytol **196:** 125–138

Yuan HM, Huang X (2016) Inhibition of root meristem growth by cadmium involves nitric oxide-mediated repression of auxin accumulation and signalling in Arabidopsis. Plant Cell Environ **39:** 120–135

Yuan HM, Xu HH, Liu WC, Lu YT (2013) Copper regulates primary root elongation through PIN1-mediated auxin redistribution. Plant Cell Physiol **54:** 766–778

Yuan TT, Xu HH, Zhang KX, Guo TT, Lu YT (2014) Glucose inhibits root meristem growth via ABA INSENSITIVE 5, which represses PIN1 accumulation and auxin activity in Arabidopsis. Plant Cell Environ **37:** 1338–1350

Zakir HA, Subbarao GV, Pearse SJ, Gopalakrishnan S, Ito O, Ishikawa T, Kawano N, Nakahara K, Yoshihashi T, Ono H, et al (2008) Detection, isolation and characterization of a root-exuded compound, methyl 3-(4-hydroxyphenyl) propionate, responsible for biological nitrification inhibition by sorghum (Sorghum bicolor). New Phytol **180:** 442–451

Zhang H, Jennings A, Barlow PW, Forde BG (1999) Dual pathways for regulation of root branching by nitrate. Proc Natl Acad Sci USA **96:** 6529–6534

Zhao Y, Christensen SK, Fankhauser C, Cashman JR, Cohen JD, Weigel D, Chory J (2001) A role for flavin monooxygenase-like enzymes in auxin biosynthesis. Science **291:** 306–309

Zheng B, Chen X, McCormick S (2011) The anaphase-promoting complex is a dual integrator that regulates both microRNA-mediated transcriptional regulation of cyclin B1 and degradation of cyclin B1 during *Arabidopsis* male gametophyte development. Plant Cell **23:** 1033–1046